UNIVERSITAT DE LES
ILLES BALEARS

Master Thesis

Updating rules and the voter model

Author:
Juan Fernández Gracia

Supervisors:
Maxi San Miguel
and Víctor M. Eguíluz

Instituto de Física Interdisciplinar y Sistemas Complejos

January 28, 2011

The dissertation of Juan Fernández Gracia is approved:

Chair Date

Date

Date

University of the Balearic Islands, The University of the Balearic Islands

Winter 2011

Updating rules and the voter model

by

Juan Fernández Gracia

THESIS

Presented to

The University of the Balearic Islands

in Partial Fulfillment

of the Requirements

for the Degree of

MASTER OF PHYSICS

February 2011

Updating rules and the voter model

A

Conchita y José María

Acknowledgements

Agradezco en primer lugar a mis directores de tesis Víctor M. Eguíluz y Maxi San Miguel por lo que me están enseñando. También quiero agradecer a los profesores de Master de Física de la UIB por los conocimientos transmitidos. A F. Vázquez por sus enseñanzas y discusión sobre el modelo del votante.
A mi compañera María, que me mete la caña que a veces me hace falta.
A mis compañerxs de doctorado en el IFISC, sino no habría calor humano. A Alex, mi poeta favorito; a Juanito, siempre dispuesto a ayudar; a Luís, que sí que sabe calcular; a Przemeck, por Polaco, que me recuerda a mi tierra y a todos los demás. A gente que he tenido la suerte de conocer como Fernando, Lucas. A Xavi, por dejar el terreno preparado.
A mi familia de Mallorca, en especial a Amparo y a Francis por acogerme.
A mis padres, que me han dado todo lo necesario para ser lo que hoy soy. A mi hermana, que me comprende. Pero sobre todo a mi abuela Juana, porque sin ella nada de todo esto habría sido posible.

Contents

Preface

Statistical physics has had already a great succes in describing how global phenomena appear, taking as point of departure a set of simple entities which interact among them. Given the general framework that it provides, there is a trend towards applying the statistical physics' techniques in interdisciplinary fields away from traditional physics such as biology, medicine, information technology and computer science among others. Social phenomena are being studied for the last years from this point of view too. In social sciences the basic units are not particles but humans. Despite humans appear to be quite heterogeneous and interact only with a small number of peers compared to the whole population, stunning global regularities appear. Examples of this are the sudden appearance of fashions, or the adoption of one of two apparently equivalent technological innovations, or the sudden massive spread of a fad, which point to the idea of studying them as disorder-order transitions. This kind of phenomena suggests the idea of studying society from the statistical physics' point of view, as it aims at explaining non trivial collective behaviors from the interaction of relatively simple indivivuals. In the past few years a lot of research has been done in this direction. The triggering facts for this were the appearance of large databases on human activities, the appearance of new social phenomena (mostly related to the internet) and the tendency of social scientist towards quantitative analysis. But a big difficulty appears. Classically, statistical physics deals with atoms and molecules, which always obbey the same laws. On the contrary humans, the basic units of society, do not behave this way. The actions of humans are already the outcome of complex physiological and psychological processes, which are largely unknown by now. But statistical physics has here also something to add. In most situations qualitative properties of large scale phenomena do not depend on the microscopic details of the process. Symmetries, dimensionality or conservation laws are sometimes the only important ingredients to have the same qualitative result irrespective of the details. This is what is called *universality*. With this concept in mind we can model society, trying to include the basic ingredients of the individuals and their interactions. A crucial step is to compare the features of the models with those of real data, to see whether the trends are similar, or we need additional ingredients to recover the same qualitative behavior.

In this work we deal with a model for consensus formation. These are models in which there is a population of agents and each of them can be in one of many equivalent states. Through interactions among the agents, they can change their states, normally converging locally. The basic questions in these kind of models are: what will be the final state, and how is the transient to this state? The interaction amongst the agents and the topology of the interactions (who interacts with whom) defines typically what the final state will be: either all agents having the same state (consensus) or coexistence of agents in the different states. There exist many of these models. Some of them are based on a random imitation process as the voter model [1, 2, 3], others incorporate the pressure that society makes on us like the majority rule model [4, 5], others incorporate what is called *bounded confidence* or *homophily*, that is the fact that individuals interact only with other individuals whose opinions are not very different from their own opinion like the Deffuant model [6], the Hegselmann-Krause model [7] or the Axelrod model [8]. As the simplest case of this type of models we choose the voter model. The agents can be in one of two equivalent states, and whenever two of the agents interact, one of them copies the state of the other one. It is an imitation interaction. The system has two absorbing states, *i.e.* states where the dynamics freezes, which correspond to consensus configurations in either of the two states.

In these kind of models persistence has been studied [9] taking into account the number of agents which have not changed state at simulation time t from a given initial condition at simulation time $t = 0$. In this work we extend this concept to measure the interevent time distribution, that is, the probability that an agent stays a certain time t without changing state. In this way we quantify the activity patterns. The extension of this kind of measure is motivated by recent measurements on human activity where the interevent time distributions were extracted. The common feature for many human activities is that the distribution of times between consecutive events has a heavy tail, where extremely long times are to be expected. When measuring it in the usual voter model this is not what is observed. We argue that the update rule, *i.e.* the order and timing by which agents are updated, is responsible for the activity patterns. The issue of the update rule and its dynamical consequences on the models has already been noticed and investigated in several studies. For example it was shown that if all agents are updated at the same time, this can result in chaotic or periodic behavior for some models, while this kind of solutions are not present for an asynchronous update [10, 11]. In order to account for heavy tails in the persistence distributions we propose an update rule and implement it in two conceptually different ways. One of the ways is coupled to the states of the agents (*endogenous update*) and the other does not (*exogenous update*). We will see that the macroscopic outcome of the model in terms of consensus formation is modified when using the endogenous update.

The organization of the manuscript is as follows. In the first chapter we define the voter model and review the previous results on it, which are for a particular standard update rule called random asynchronous update (RAU). In the second chapter we define standard update rules used in simulations of agent based models and study the voter model with those update rules in terms of consensus, but quantifying also the activity patterns by measuring the persistence distribution, *i.e.* the distribution of times between consecutive changes of state of the single agents. In terms of consensus, the model does not order for the networks studied. Concerning the activity patterns, they are quite homogeneous, with the persistence distribution showing an exponential tail. In the third chapter we present a new update rule and apply it to the voter model in two different ways. The *exogenous update*, which is decoupled from the dynamics, gives rise to changes in the timescales, but qualitatively the same behavior as with standard update rules. The *endogenous update*, which is coupled to the states of the agents, leads to a coarsening process which orders the system. The activity patterns are modified by the new update rule and we find persistence distributions with power-law tails. The fourth chapter contains the conclusions of the work. There is one appendix in the end, which explains briefly the interaction networks (who interacts whith whom) that were used for computer simulations in the second and third chapters.

1

The Voter Model

1.1 Definition of the voter model

The voter model is a microscopic model born in the theory of probabilities [1]. It was named in this way for the natural interpretation of its rules in terms of opinion dynamics [12, 13], however it has been investigated not just in the context of social dynamics but also in fields such as probability theory [1] and population dynamics [14]. It was first considered in Ref. [14] in 1973 as a model for the competition of species and named *voter model* in Ref. [1] in 1975.
It consists of a set of N agents placed on the nodes of an interacting network. The links of the network are the connections among agents. Two nodes are first neighbours if they are directly connected by a link in the network. The agents have a binary variable (opinion, state,...) which can take the values $+1$ or -1. The behaviour of the agents is characterized by an imitation process, because, whenever they interact, they just copy the state of a randomly chosen first neighbour.
The model has two absorbing configurations, *i.e.*, configurations in which the dynamics stop, which consist either of all agents in state $+1$ or in state -1. These absorbing configurations are also typically called *consensus*, as the whole population has agreed in the same state.
This model has been studied by computer simulations using what we later define as *random asynchronous update* for node dynamics. In this case the basic steps in the dynamics are:

1. Randomly choose an agent i with opinion x_i.

2. Randomly choose one of i's neighbours, j, with opinion x_j. Agent i adopts j's opinion; $x_i \to x_i = x_j$.

3. Repeat *ad infinitum*.

The alternative link dynamics considered in Ref. [2] is defined by the following steps:

1. Randomly choose a link $i - j$.

2. i adopts j's opinion with probability 1/2 ($x_i \to x_i = x_j$). Otherwise j adopts i's opinion ($x_j \to x_j = x_i$).

3. Repeat *ad infinitum*.

For regular networks, where every agent has the same degree, *i.e.*, the same number of neighbours, *link dynamics* is equivalent to node dynamics, but for heterogeneous networks these two updates are not equivalent [2]. Usually the time is measured in units of N basic steps, *i.e.*, a montecarlo step, following the idea that every agent gets updated on average once per unit time.

1.1.1 Macroscopic description

A basic question is under which conditions consensus will be reached and how. In order to answer this question we have to define some macroscopic quantities which will describe the state of the system and its dynamical behaviour.

Magnetization $m(t)$: It is a quantity that reflects the configuration of the system as a whole. It is just the average state of the population and is defined as

$$m(t) = \frac{1}{N} \sum_{i=1}^{N} x_i.$$

Density of interfaces $\rho(t)$: This quantity characterizes locally the level of order in the system. It is the density of links in the network connecting agents with different states. This is a good quantity to use as order parameter as it is nonzero while the system is not in one of the absorbing states and is zero otherwise. It is defined as

$$\rho(t) = \frac{\text{\# of links between } -1 \text{ and } +1}{\text{\# of links in the network}} = \frac{1}{\sum_{i=1}^{N} k_i} \left(\sum_{\langle ij \rangle} \frac{1 - x_i x_j}{2} \right),$$

where $\langle ij \rangle$ stands for summing over neighbouring nodes. A decrease of $\rho(t)$ describes the coarsening process with growth of domains with agents in the same state.

In numerical simulations of the voter model finite size effects come into play. In finite size systems consensus will be reached, but we have to diferentiate if consensus is reached due to the inherent dynamics or to a finite size fluctuation. We use averages over many realizations to extract the mean behaviour. This is what is called an ensemble average and will be denoted by $\langle \cdot \rangle$. When doing the ensemble averages some conservation laws can be found. For the case of regular networks, where every node has the same number of neighbours (same degree), the ensemble average of the magnetization $\langle m(t)\rangle$ is conserved under node dynamics [2]. For this reason the magnetization is not a good order parameter and we have to define the density of interfaces ρ, which in general is not conserved. But if the network is heterogeneous, *i.e.*, the degrees of the nodes are not all the same, the conservation law for $\langle m(t)\rangle$ breaks down unless we use link dynamics. If we use node dynamics we can still find a conserved quantity, which is an ensemble average of a magnetization weighted with the degree k_i of node i [2].

$$m'(t) = \frac{\sum_{i=1}^{N} k_i x_i}{\sum_{i=1}^{N} k_i}. \tag{1.1}$$

Notice that, when doing link dynamics we are in fact choosing a node for being updated with probability proportional to its degree.

In order to gain more insight into the dynamics for finite size systems we also introduce two other quantities to characterize the dynamics. These quantities are:

Survival probability $S(t)$: It is the probability that a realization of the system has not reached one of the absorbing states at time t. The mean time $\langle T\rangle$ to reach consensus is then given by[1]

$$\langle T\rangle = \int_0^\infty S(t)dt.$$

Density of interfaces averaged over surviving runs $\langle\rho^*(t)\rangle$: This quantity is basically the same as the density of interfaces, but disregarding the realizations that have already reached an absorbing state when doing the ensemble average. It tells us the degree of order in the system for the realizations that are still in an active state. This quantity is related to the density of interfaces averaged over all realizations by

$$\langle\rho(t)\rangle = S(t)\langle\rho^*(t)\rangle.$$

1.2 Summary of results

The voter model has been investigated on many different interaction networks ranging from regular lattices to different kinds of complex networks [2, 15, 3, 16]. Conservation laws have been found [2, 17] and theoretical calculations on the dynamical behaviour of the model have also been reported [18, 19, 20, 21]. A review on this model as well as other social dynamics investigations can be found in Ref. [13].

[1] $S(t)$ is the probability of being in an active configuration at simulation time t. Then the probability of reaching an absorbing state at time t is $d/dt(1 - S(t)) = -d/dtS(t)$. The average time to reach consensus is then $\langle T\rangle = -\int_0^\infty (tdS(t)/dt)dt$ and, integrating by parts one finds that $\langle T\rangle = \int_0^\infty S(t)$.

1.2.1 Hypercubic lattices

Microscopic models in Statistical Mechanics have been historically studied on regular lattices [22, 23, 24]. d-dimensional regular lattices are topologies where every node has the same number of connections such that it is discrete translational invariant in the d directions. For example in one dimension what we have is a chain. In the simplest case any node in the chain has only two connections, but there could be more connections. In two dimensions there are more possibilities, as one can build a square lattice, a triangular lattice, a honeycomb,...

Hypercubic lattices in one dimension are square lattices, in three dimensions are simple cubic lattices and so on. For hypercubic lattices of arbitrary dimension the model is solvable. In early studies by probabilists [14, 25, 1, 26] the fact that the model can be exactly mapped on a model of random walkers that coalesce upon encounter was exploited. Then, using the machinery of random walk theory [26, 27] the model can be solved. We will follow instead another approach based on master equations to derive the general solution on lattices, see Ref. [28]. Considering a d-dimensional square lattice and being $X = \{x_i, i = 1, \ldots, N\}$ the configuration of the system, the transition rate for an agent k to change state is

$$W_k(X) = \frac{d}{4}\left(1 - \frac{1}{2d} x_k \sum_j x_j\right), \tag{1.2}$$

where j runs over all $2d$ nearest neighbours and the prefactor that sets the overall timescale is chosen for convenience. The probability of having configuration X at time t, $P(X, t)$, obeys the master equation

$$\frac{d}{dt}P(X,t) = \sum_k [W_k(X^k)P(X^k,t) - W_k(X)P(X,t)], \tag{1.3}$$

where X^k is equal to X except for the agent with changed state x_k. Due to the particular form of the transition rates , Eq. (1.2), the equations for correlation functions of any order $\langle x_k \cdots x_l\rangle = \sum_X P(X,t)x_k \cdots x_l$ can be closed, *i.e.*, they do not depend on higher order functions and hence can be solved. The equation for the mean value of the state of an agent is

$$\frac{d}{dt}\langle x_i\rangle = \Delta_i \langle x_i\rangle, \tag{1.4}$$

where Δ_i is the discrete Laplace operator. Summing over i one sees that the ensemble average of the magnetization $\langle m(t)\rangle$ is conserved. This conservation allows us to determine the probability that a finite size system will end with all agents in state $+1$ or -1 (exit probability), depending on the initial configuration of the system. The probability of ending with all agents in state $+1$ is equal to the initial fraction of agents in that state. For the two-body correlation function we have

$$\frac{d}{dt}\langle x_k x_l\rangle = (\Delta_k + \Delta_l)\langle x_k x_l\rangle. \tag{1.5}$$

The structure of this equation is similar [28] in any dimension to the equations of the one-dimensional Ising model with zero temperature Glauber dynamics [29], which is equivalent to the voter model in one dimension. It can be solved via Laplace transform. In this way we can know the asymptotic behaviour of the density of interfaces $\langle\rho(t)\rangle = (1 - \langle x_k x_{k+1}\rangle)/2$ [28]

$$\langle\rho(t)\rangle \propto \begin{cases} t^{-(2-d)/2} & d < 2 \\ 1/\ln(t) & d = 2 \\ a - bt^{-d/2} & d > 2. \end{cases} \tag{1.6}$$

This shows that for $d \leq 2$ the voter model undergoes a coarsening process leading to complete consensus, while for $d > 2$, and in the thermodynamic limit, it has asymptotically a finite density of interfaces and thus no consensus is reached. This means that $\langle\rho(t)\rangle$ stays asymptotically at a plateau (the constant value a in Eq. (1.6)). However, as mentioned before, for finite size systems consensus is reached invariably. In this case, for long times $\langle\rho(t)\rangle$ departs from Eq. (1.6) with an exponential decay. One can extract the time T_N needed to reach consensus in a system of size N [30]

$$T_N \propto \begin{cases} N^2 & d = 1 \\ N\ln(N) & d = 2 \\ N & d > 2. \end{cases} \tag{1.7}$$

We emphasize that the way consensus is reached on finite systems has a different nature for $d \leq 2$, where the system tends towards consensus by a coarsening process, and for $d > 2$, where a large fluctuation takes the system to the absorbing configuration. In Fig.1.1 one can see the evolution of $\langle\rho(t)\rangle$ for different system sizes of one dimensional and two dimensional cubic lattices. The evolution is as stated in Eq. (1.6) until a finite size fluctuation brings the system to the absorbing configuration before the coarsening process ends.

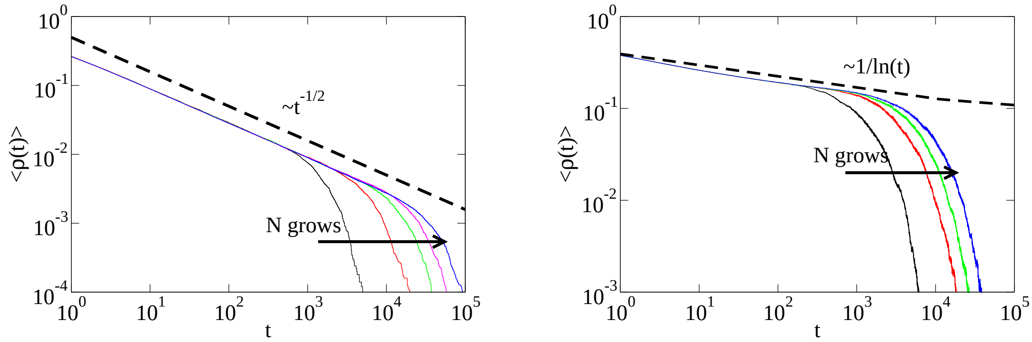

(a) Time evolution of the density of interfaces averaged over all runs for a one dimensional system. The dashed line corresponds to a power-law decay with exponent $-1/2$. The system sizes are $N = 100, 200, 300, 400, 500$.

(b) Time evolution of the density of interfaces averaged over all runs in a log-log plot for a two dimensional system. We can see that the system coherently goes toward consensus following a law $\propto 1/\ln(t)$. The system sizes are $N = 30^2, 50^2, 60^2, 70^2$.

Figure 1.1: Time evolution of the density of interfaces for regular lattices in one and two dimensions, where the system reaches consensus by a coarsening process (Eq. 1.6). All the curves are averages over 1000 realizations of the dynamics with random initial condition with, on average $\langle m(0)\rangle = 0$.

1.2.2 Complete graph

In a complete graph every agent in the network is connected to every other agent. It is also called *all-to-all* interaction. The model can be solved using a master equation approach [15, 21] for the probability density $P(m, t)$ of having magnetization m at time t. The equations for the averaged quantities $\langle m(t)\rangle$ and $\langle \rho(t)\rangle$ in finite systems are respectively [18]

$$\frac{d}{dt}\langle m(t)\rangle = 0, \tag{1.8}$$

$$\frac{d}{dt}\langle \rho(t)\rangle = -\frac{2}{N-1}\langle \rho(t)\rangle. \tag{1.9}$$

From the conservation of the magnetization, Eq. (1.8) and knowing that all realizations of the model on a finite systems finally reach one of the absorbing configurations, we can infer the exit probability, *i.e.*, the probability that the systems ends in the absorbing configuration $+1$ or -1. The probability of ending in each one of the absorbing configurations is equal to the initial fraction of agents in that state, $P(m = \pm 1, t \to \infty) = \frac{1\pm m(0)}{2}$. (The same argument that we did for the case of regular lattices.)
From Eq. (1.9) for the evolution of the average density of interfaces we know that in a finite system it will behave as an exponential with a characteristic time $\tau(N) = (N-1)/2$. In the thermodynamic limit, *i.e.*, in the infinite system size

limit, we see that the average density of interfaces also remains constant and equal to its initial value due to the divergence of $\tau(N)$. This is a state that is only stable in the thermodynamic limit. For finite size systems it is a metastable state, around which the system is trapped.
In order to gain more insight, let us separately consider the survival probability $S(t)$ and the density of interfaces averaged over surviving runs.
The survival probability is calculated in Refs. [21, 18] and, for $m(0) = 0$ it is

$$S(t) = \begin{cases} 1 & t \ll \tau(N) \\ \frac{3}{2} e^{-t/\tau(N)} & t \gg \tau(N), \end{cases} \tag{1.10}$$

where $\tau(N)$ is the same as before. Then, using the relation $\langle \rho(t) \rangle = S(t) \langle \rho^*(t) \rangle$, the density of interfaces averaged over surviving runs is easily computed

$$\langle \rho^*(t) \rangle = \begin{cases} \frac{1}{2} e^{-t/\tau(N)} & t \ll \tau(N) \\ \frac{1}{3} & t \gg \tau(N). \end{cases} \tag{1.11}$$

We realize that the fully ordered state is not reached in the thermodynamic limit. There are two reasons for drawing this conclusion. On the one hand the temporal scale $\tau(N)$ over which consensus is reached in finite systems diverges with the system size N. This is already evident from the behaviour of $\langle \rho(t) \rangle$, which will remain constant and equal to its initial value. On the other hand we see that even for $t \gg \tau(N)$ the fraction of interfaces in surviving runs is finite independent of the system size. This means that surviving runs do not order but stay in configurations with, on average, a finite fraction of interfaces. The plateau observed in this quantity differs from the one in $\langle \rho(t) \rangle$ for the infinite size limit because, when doing the average over surviving runs, the fluctuations around the metastable state are not symmetric, but can only go below it. A random fluctuation will eventually bring the system to consensus, but as long as a realization survives, it stays, on average, in a disordered configuration. The decay of $\rho(t)$ is then a consequence of the decay in the survival probability $S(t)$.
In Fig. (1.2) we show the evolution of the ensemble average of $\rho(t)$ (Figs.1.2a and 1.2b) on a complete graph in different scales. The log-log plot shows better the existence of a plateau (dashed line) in the thermodynamic limit, while the log-linear plot makes clear the exponential decay. Fig. 1.2c shows the average of ρ over surviving runs, which reaches a plateau (dashed line). The last figure (1.2d) shows the evolution of ρ in a single realization. There we can see that the system is in fact trapped around the plateau (dashed line) and a big finite size fluctuation brings it to one of the absorbing configurations. Note that the fluctuations around the plateau are not symmetric and can only go below it, giving rise to a lower plateau when averaging over surviving runs (Fig. 1.2c).

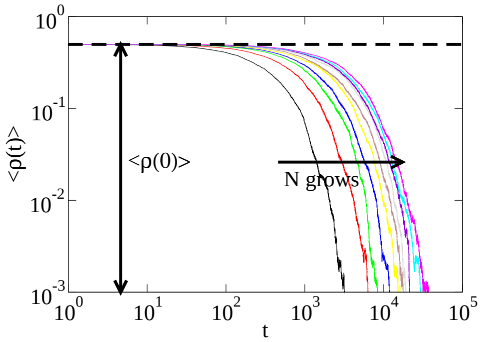

(a) Density of interfaces averaged over all runs in a log-log scale. The dashed line corresponds to the value of the plateau that will exist only in the infinite size limit.

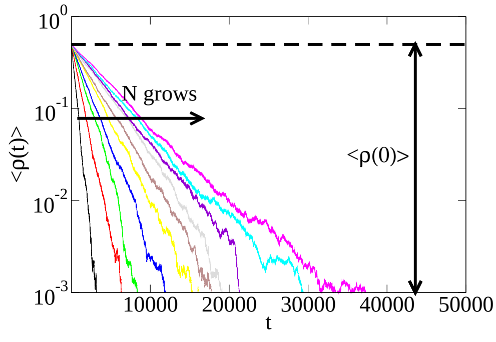

(b) Density of interfaces averaged over all runs in a log-linear scale. The exponential decay has a characteristic time that increases with the system size.

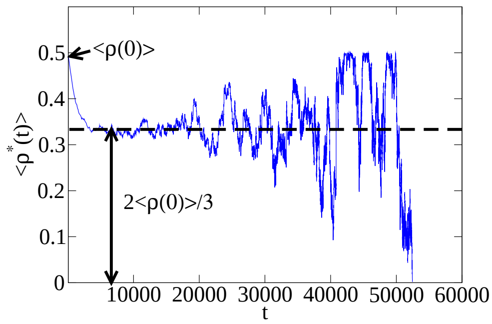

(c) Density of interfaces averaged only over surviving runs. We see that the realizations that have not reached an absorbing configuration, stay trapped in a disordered configuration. The system has $N = 10000$ agents.

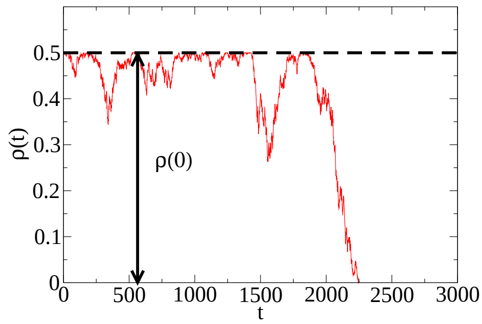

(d) Density of interfaces in a single run. The density of interfaces stays around the value corresponding to the metastable state at $\rho(0)$. Fluctuations can only go below that value. The system has $N = 5000$ agents.

Figure 1.2: Different visualizations of the density of interfaces on a complete graph. All the curves are averages over 1000 realizations of the system. The system sizes range from $N = 10^3$ to $N = 10^4$.

1.2.3 Complex networks

Random uncorrelated networks

By random uncorrelated networks we mean networks with an arbitrary degree distribution P_k[2], but no correlations between the degrees of the nodes. In fact these are families of networks, all of them having the same degree distribution. When doing simulations on them one has not only to average over many realizations, but also over different realizations of the network. Examples of such networks are the

[2] P_k is the probability that a randomly chosen node in the network has degree k.

Erdös-Renyi network [31], which consist of a set of nodes and every link that could connect any two nodes is present with certain probability p. Scale-free networks [31] can also be put into this class of networks if we retain the power-law degree distribution that gives the name to these networks, but drop any correlations between nodes' degrees. There exist methods to create networks with a given degree distribution, but random in the rest of characteristics [32].
Vázquez and Eguíluz in Ref. [18] studied the dynamics of the voter model on such networks with great detail, deriving a complete analytical description, using the fact that the degrees of the nodes are uncorrelated. The time evolution of $\rho(t)$ in an infinite size system is found to be

$$\frac{d}{dt}\rho(t) = \frac{2\rho(t)}{\langle k\rangle}\left[(\langle k\rangle - 1)\left(1 - \frac{2\rho(t)}{1 - m^2(t)}\right) - 1\right], \tag{1.12}$$

where $\langle k\rangle = \sum_{k=1}^{N} kP_k$ is the average degree of the network. From this equation we can infer that there are two stationary solutions. For $\langle k\rangle \leq 2$, the stable solution $\rho = 0$ corresponds to a fully ordered state, but this is an artifact of the approximation, since there is no abrupt change of behavior of ρ for this $\langle k\rangle$ [19]. For $\langle k\rangle > 2$, one can do an adiabatic elimination of the fast vartiable ρ, since ρ evolves much faster than m and so $\rho(t)$ accomodates to the value

$$\rho(t) = \xi(\langle k\rangle)(1 - m^2(t)). \tag{1.13}$$

This solution with

$$\xi(\langle k\rangle) = \frac{\langle k\rangle - 2}{2(\langle k\rangle - 1)}, \tag{1.14}$$

corresponds to a partially ordered system, composed by a fraction $\rho > 0$ of interfaces, as long as $m \neq \pm 1$. Notice that for networks of arbitrary degree distribution the average magnetization is not generally conserved. But if the initial distributions of $+1$ and -1 are not correlated with the degree of the nodes, then the magnetization will also be conserved when averaging over initial conditions. So with this condition we can say that in an infinite size system, the density of interfaces will evolve until it reaches the value $\xi(\langle k\rangle)(1 - m^2(0))$ and will stay there forever. This means that in the thermodynamic limit the system is not ordering.
For the case of finite systems the average density of interfaces decays rapidly to the value where it would stay in the infinite size limit and from there begins an exponential decay that can be calculated [18]

$$\langle\rho(t)\rangle = \xi(\langle k\rangle)(1 - \langle m^2(0)\rangle)e^{-t/\tau}, \tag{1.15}$$

where the characteristic time τ is

$$\tau = \frac{(\langle k\rangle - 1)\langle k\rangle^2 N}{2(\langle k\rangle - 2)\langle k^2\rangle} \tag{1.16}$$

with $\langle k^2\rangle = \sum_k k^2 P_k$ the second moment of the degree distribution. The time to reach consensus can be calculated using an analogy with random walks [18]. This

time is equal to the characteristic time τ of Eq. (1.16) times a function of the initial magnetization. This shows that the time to reach consensus scales as the system size N for any network with first moment, $\langle k \rangle$, and second moment, $\langle k^2 \rangle$, of the degree distribution independent of the system size. For the case of scale-free networks, where the second moment $\langle k^2 \rangle$ of the degree distribution depends on the system size, Eq. (1.16) is still valid, but the scaling of τ with the system size N is different [18, 20].
For a scale-free degree distribution $P_k \propto k^{-\gamma}$

$$\tau \propto \begin{cases} N & \gamma > 3, \\ N/\ln N & \gamma = 3, \\ N^{2(\gamma-2)/(\gamma-1)} & 2 < \gamma < 3, \\ (\ln N)^2 & \gamma = 2, \\ \mathcal{O}(1) & \gamma < 2 \end{cases} \tag{1.17}$$

The survival probability is:

$$S(t) = \begin{cases} 1 & t \ll \tau \\ \frac{3}{2}(1 - \langle m^2(0) \rangle) e^{-t/\tau} & t \gg \tau. \end{cases} \tag{1.18}$$

From this solution and the one for $\langle \rho(t) \rangle$ it is straightforward to recover the density of interfaces averaged over surviving runs

$$\langle \rho^*(t) \rangle = \begin{cases} \frac{(\langle k \rangle - 2)}{2(\langle k \rangle - 1)}(1 - \langle m^2(0) \rangle) e^{-t/\tau} & t \ll \tau \\ \frac{(\langle k \rangle - 2)}{3(\langle k \rangle - 1)} & t \gg \tau. \end{cases} \tag{1.19}$$

Summing up, the behavior of the voter model on uncorrelated random graphs is very similar to the behavior on a complete graph, with the times rescaled by a constant that depends just on $\langle k \rangle$ and $\langle k^2 \rangle$, and the plateau heights depending now on $\langle k \rangle$. In fact the case of a complete graph is obtained in the limit $\langle k \rangle \to \infty$. The results of computer simulations for the case of a random network with average degree $\langle k \rangle = 8$ and a scale-free graph with $\langle k \rangle = 6$ are plotted in Figs. 1.3 and 1.4 respectively. The figures contain similar plots to those presented for the case of a complete graph (figure 1.2). In Fig. 1.5 Eq. (1.14) for the height of the plateau is tested against computer simulations, showing good agreement.

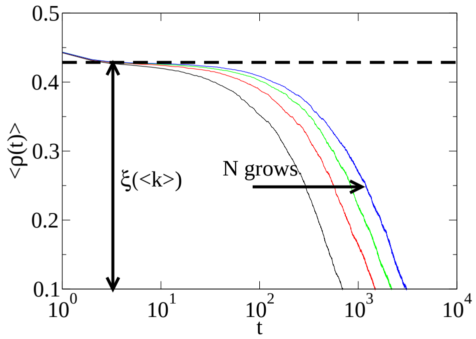

(a) Density of interfaces averaged over all runs in linear-log scale. The dashed line shows the value of the plateau that will exist only in the infinite size limit.

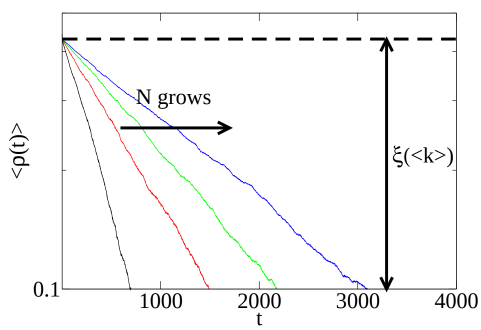

(b) Density of interfaces averaged over all runs in log-linear scale. The exponential decay has a characteristic time that increases with the system size and diverges in the infinite size limit.

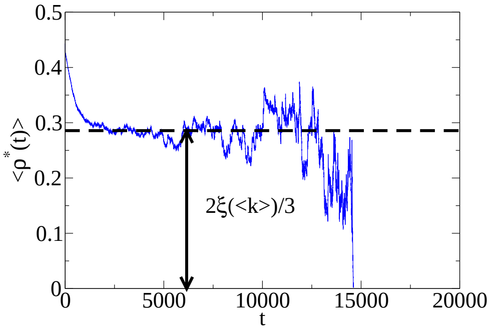

(c) Density of interfaces averaged only over surviving runs. The realizations that have not reached an absorbing state, stay trapped in a disordered state. The system has $N = 4000$ agents.

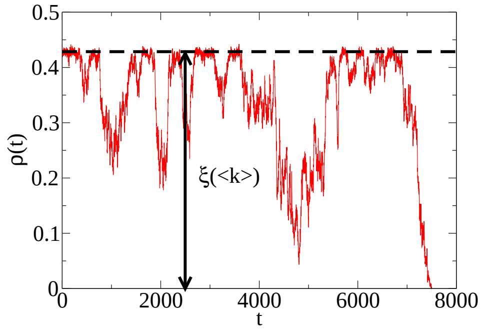

(d) Density of interfaces in a single run. The density of interfaces stays around the value corresponding to the metastable state at $\xi(\langle k\rangle)$. Fluctuations can only go below that value. The system has $N = 4000$ agents.

Figure 1.3: Different visualizations of the density of interfaces on an Erdös-Renyi random graph with average degree $\langle k\rangle = 8$, *i.e.* $\xi(\langle k\rangle) = 3/7$. All the curves are averages over 1000 realizations of the system. The system sizes range from $N = 10^3$ to $N = 4 \cdot 10^3$. The initial magnetization is $m = 0$.

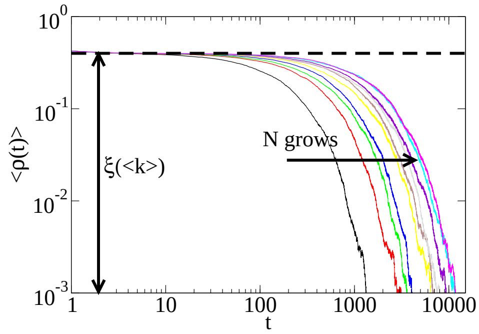

(a) Density of interfaces averaged over all runs in log-log scale. The dashed line corresponds to the value of the plateau that will exist only in the infinite size limit.

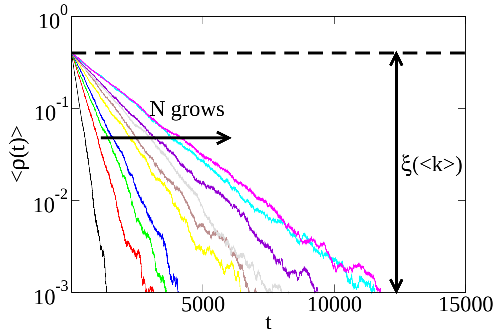

(b) Density of interfaces averaged over all runs in log-linear scale. The exponential decay has a characteristic time which increases with the system size and diverges in the infinite size limit.

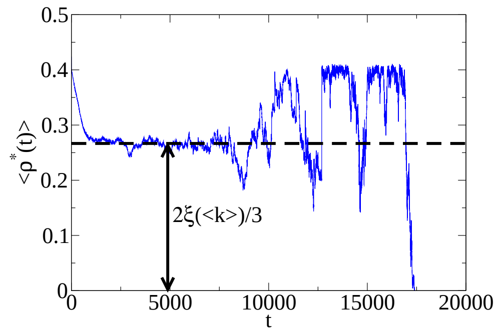

(c) Density of interfaces averaged only over surviving runs. We see that the realizations that have not reached an absorbing state, stay trapped in a disorder state. The system has $N = 10000$ agents.

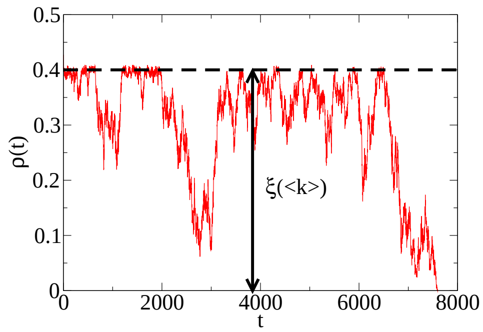

(d) Density of interfaces in a single run. The density of interfaces stays around the value corresponding to the metastable state at $\xi(\langle k \rangle)$. Fluctuations can only go below that value. The system has $N = 10000$ agents.

Figure 1.4: Different visualizations of the density of interfaces on a Barabási-Albert scale-free graph ($P_k \propto k^{-3}$) with average degree $\langle k \rangle = 6$, *i.e.* $\xi(\langle k \rangle) = 2/5$. All the curves are averages over 1000 realizations of the system. The system sizes range from $N = 10^3$ to $N = 10^4$. The initial magnetization is $m = 0$.

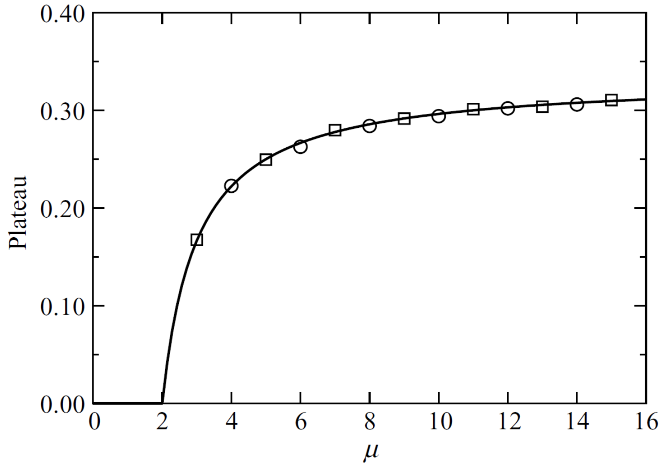

Figure 1.5: Plateau heights of ρ^* as a function of $\langle k \rangle$ (labeled μ in the figure). Circles are for Barabási-Albert scale-free networks and squares for degree regular random networks [3], both of size $N = 10^4$. The solid line is the analytical prediction $2\xi(\langle k \rangle)/3 = \frac{(\langle k \rangle - 2)}{3(\langle k \rangle - 1)}$. From Ref. [18].

Small-World networks

In the literature one can find two definitions of the *small-world* property of networks. Sometimes it is defined as the characteristic of a network, whose average shortest path length connecting two nodes in the network is very small compared to the size of the network. The other definition is the previous characteristic plus a high clustering coefficient, which translates in a high probability that two neighbours of a node are also neighbours between them.
In the sense of the second definition, Watts and Strogatz in Ref. [33] proposed a model for generating networks with both properties. These networks are called *small-world networks*. Their model consists of a regular network in one dimension with periodic boundary conditions (a ring), where each node connects to k nearest neighbours. Each link in the network is rewired with certain probability p. By varying p between 0 and 1 we interpolate between a regular one-dimensional network and a random network. For intermediate values of p the small-world regime is found, where the average shortest path length is very small compared to the system size and the clustering coefficient very high compared to the one obtained for a random network of the same size.
The behaviour of the voter model on these networks was studied numerically in Ref. [16] and later analytically in Ref. [34]. The presence of long-range connections inhibit the ordering process in the thermodynamic limit, which is a counterintuitive result. A metastable dynamical state with coexisting opinions is found. There exist

[3] Degree regular random networks are such that each node in the system has the same degree, but there are no other correlations. So the nodes are linked at random taking into consideration two constraints: the degree is the same for all nodes and there are no repeated links.

two different times cales. When the average size of a growing domain, which has a size $\xi \sim 1/\rho$ in one dimension, is much smaller than the characteristic length between two shortcuts, $l^* = 1/(kp)$ [35], the coarsening process is practically $\rho \propto t^{-1/2}$; as in a one-dimensional lattice. When $\xi \sim l^*$, the long range interactions start to play a role, and the coarsening stops: ρ reaches a plateau [16] and in the thermodynamic limit the absorbing state is never reached. This is different in finite size systems, where finite size effects eventually drive the system to an absorbing state, and the time to reach it scales as $T \propto N$. In Fig. 1.6 the time evolution of the average density of interfaces $\langle \rho(t) \rangle$ is plotted for small world networks and for a one dimensional ring for different system sizes.

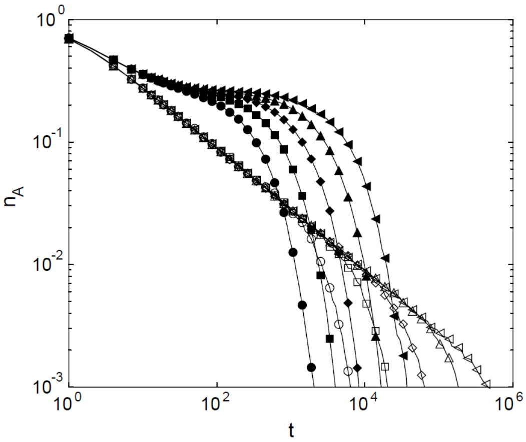

Figure 1.6: Time evolution of the average density of interfaces $\langle \rho(t) \rangle$ (labeled n_A in the figure). Values are averaged over 1000 realizations. Time is measured in Monte Carlo steps per site. Empty symbols are for the one-dimensional case ($p = 0$). Filled symbols are for rewiring probability $p = 0.005$. Data are for $N = 200$ (circles), $N = 400$ (squares), $N = 800$ (diamonds), $N = 1600$ (triangles up) and $N = 3200$ (triangles left). From Ref. [16].

Other effects of different characteristics of the network of interaction have been studied. For example Suchecki *et al.* in Ref. [3] studied in great detail the effect of different characteristics of heterogeneous networks on the plateau heights of the metastable states and the survival times. The results presented come to support the claim that whether the system orders under the rules given by the voter dynamics depends on the effective dimensionality of the interaction network. In any complex network, which in general has an effective infinite dimension, the dynamics gets trapped in metastable states. In finite systems one of the absorbing states is reached by finite size fluctuations that bring the system out of the metastable state. As an example of the crucial role of dimensionality the authors of Ref. [3] checked that the coarsening process in a scale-free network with effective dimension equal to one was the same as in a regular network of dimension one, *i.e.*, $\langle \rho(t) \rangle \propto t^{-1/2}$.

2

Standard update rules

In this chapter we review standard update rules used in simulations of agent based models (ABM's). We also investigate the behavior of the voter model for these different rules. In ABM's agents are placed on the nodes of a network. The state of the agents is characterized by a variable that can take one of various values. The specific dynamics tells how the states of the nodes are updated. But in addition to the dynamical rules, simulation incorporate rules that determine when an agent is given the opportunity to update her state. Standard update rules implement a homogeneous pattern of updates in time.

The simulations all over this and the next chapter where done with random initial conditions, *i.e.* every agent has the same probability in the beginning to have one state or the other, and setting their persistence time equal to zero, *i.e.* the time since their last change of state.

2.1 Definitions of standard update rules

Typically the update rules implemented are

- **Asynchronous update:** At each simulation step only one of the agents is updated. The unit of time is typically defined as N simulation steps (a montecarlo step), where N is the number of agents in the system.

  Random asynchronous update (RAU): the agents are updated in a random order (*cf.* Fig. (2.1)).

  Sequential asynchronous update (SAU): the agents are always updated in the same order (*cf.* Fig. (2.2)).

- **Synchronous update (SU):** All the agents are updated at the same time. The time is measured in units of simulation steps (*cf.* Fig. (2.3)).

In the previous chapter we reviewed the results of the voter model under RAU, which is the update rule most commonly used in simulations of the voter model.

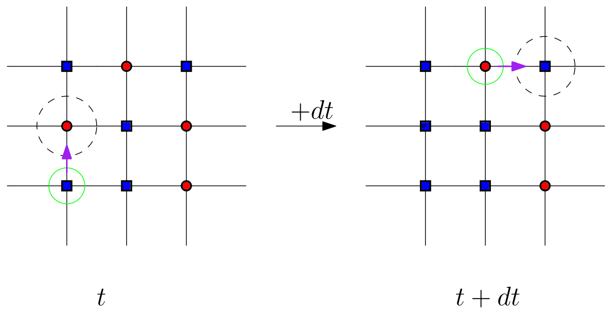

Figure 2.1: Example of random asynchronous update, RAU. For each $dt = 1/N$ one randomly picked agent is updated.[1]

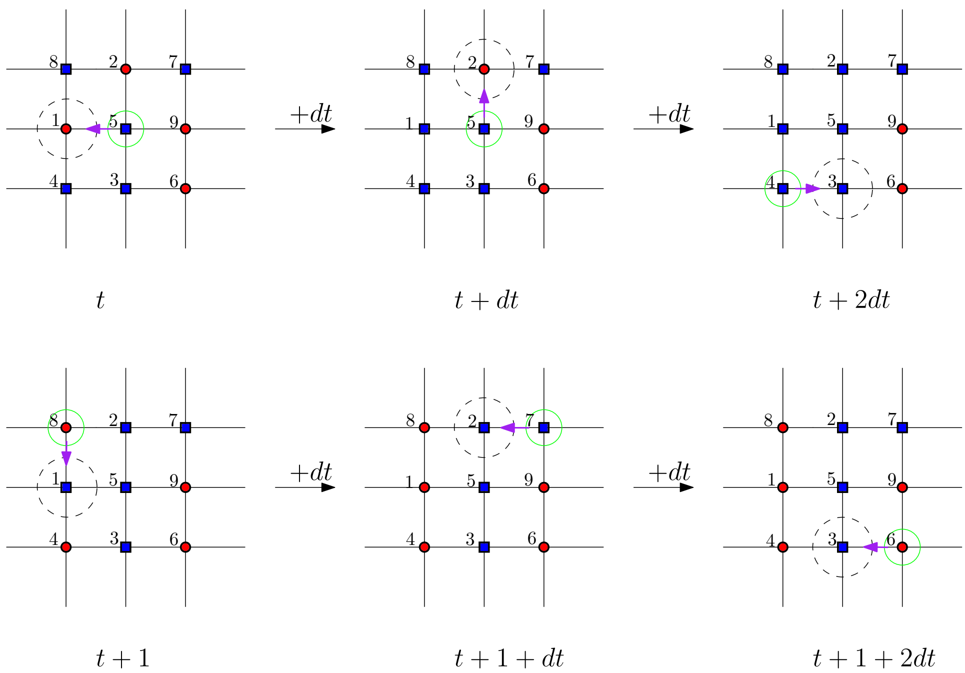

Figure 2.2: Example of sequential asynchronous update, SAU. Remember that $dt = 1/N$. The agents are updated always in the same order, so after a time delay of 1 the same agent is updated.[1]

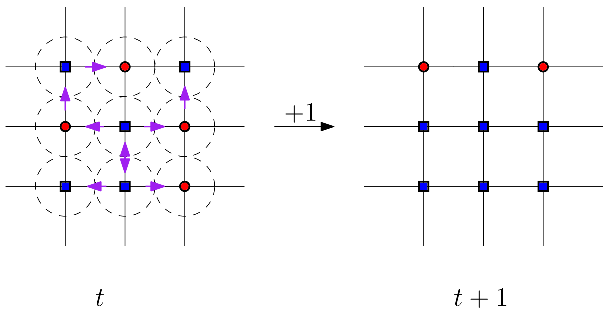

Figure 2.3: Example of synchronous update, SU. All agents are updated at the same time.[1]

As we can see from the definitions of these standard update rules, there exists a well defined characteristic time between two consecutive updates of the same node. In the case of SAU and SU every agent is updated exactly once per unit time, while for RAU this only happens on average.
In the cellular automata literature the topic of the update rules used in simulations has been widely studied (see for example [36, 37, 38, 39, 40, 11]). Different update rules may result in very different collective behavior. In particular SU on regular lattices can result in periodic or chaotic patterns in time coming from the inherent discrete dynamics, like maps. These behaviours do not have their counterpart when dealing with other update rules. This was found for the case of the spatial prisoner's dilemma in [10] and explained later in [11]. In the case of the voter model under SU in a regular lattice periodic behavior is found if the system reaches a configuration that is chess-board like (*cf.* Fig. (2.4)). The whole system stays indefinitely switching between two configurations. When comparing different update rules for the voter model we will avoid this situation by running the simulations on disordered networks of effective infinite dimensionality (see appendix A).

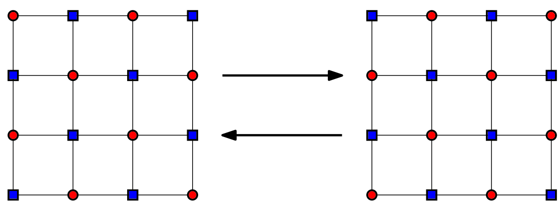

Figure 2.4: Example of dynamical trap in the dynamics of the voter model for SU on a two dimensional square lattice. The state of the system alternates between both states.

[1]In these figures we exemplify the diferent kinds of update rules for the voter model on a two dimensional square lattice. The two possible states of the nodes are represented by blue squares and red circles. The node or nodes inside a black dashed circle are the ones that are updated. The nodes inside a green circle are the randomly chosen neighbours for the interaction and the purple arrow tells in which direction the state will be copied.

2.2 Voter model with standard update rules

In this section we report simulations of the voter model under SAU and SU node update dynamics and compare the results with the ones reviewed in section 1.2 for RAU node update dynamics.
In Figs. 2.5-2.7 we can see the outcome of the simulations on a complete graph (Fig. 2.5), a random graph of average degree $\langle k \rangle = 6$ (Fig. 2.6) and on a scale-free graph of average degree $\langle k \rangle = 6$ (Fig. 2.7). These figures include plots of the averaged density of active links $\langle \rho(t) \rangle$, the density of active links averaged only over surviving runs $\langle \rho^*(t) \rangle$, the evolution of ρ in a single realization, the survival probability $S(t)$ and the cumulative persistence $C(\tau)$. The cumulative persistence is a quantity which we did not consider in chapter 2 and it is used to characterize the activity patterns paying attention to the interevent times in a realization of the voter model. We define interevent time as the time elapsed between two changes of state of a single agent. We extract the interevent cumulative distribution, or cumulative persistence $C(\tau)$ from the simulations. From this distribution we can compute the probability density of interevent times (persistence) $M(\tau)d\tau = -dC(\tau)$. This distribution describes the activity patterns of change of state. The question of interest is if $M(\tau)$ is Poisson-like or a more heterogeneous distribution.
Results for RAU, SAU and SU are plotted together in Figs.2.5-2.7 for comparison purposes. We observe that the averaged density of active links $\langle \rho(t) \rangle$, the survival probability $S(t)$ and the tail of the cumulative persistence $C(\tau)$ display an exponential decay $\exp(-t/\tau(N))$, with a characteristic time that depends on the system size. These characteristic times have been extracted by fitting the data for many system sizes and computing the scaling behaviour of $\tau(N)$. The results of this data analysis is summarized in table (2.1) for the different update rules and networks. For $\langle \rho(t) \rangle$ and $S(t)$ the same characteristic time is found. By inspecting the figures we can realize that those characteristic times have to be the same in order to get the plateau in the density of active links averaged over surviving runs shown in Figs. 2.5c,2.6c,2.7c, as $\langle \rho^*(t) \rangle = \langle \rho(t) \rangle / S(t)$.

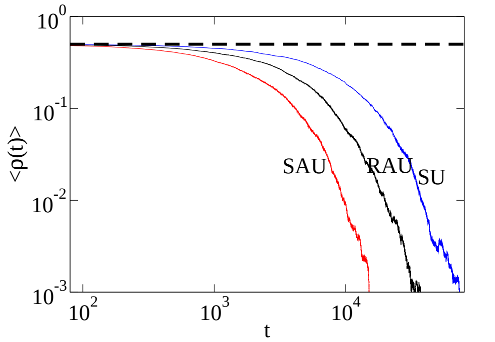

(a) Density of active links averaged over all runs in log-log scale. The dashed line corresponds to the plateau that will exist only in the thermodynamic limit.

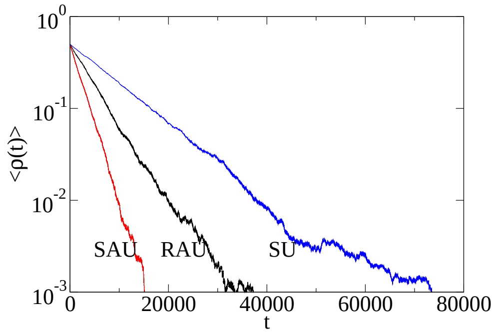

(b) Density of active links averaged over all runs in log-linear scale.

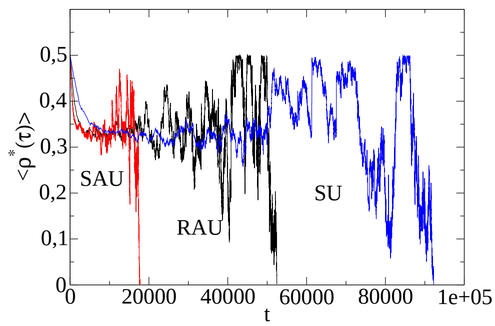

(c) Density of active links averaged over surviving runs.

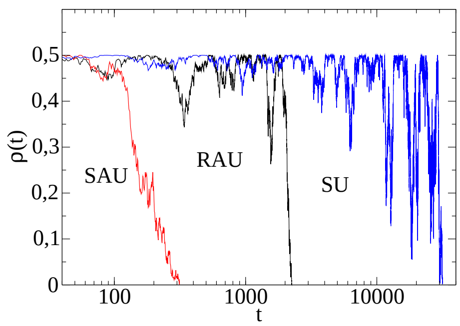

(d) Density of active links in single realizations.

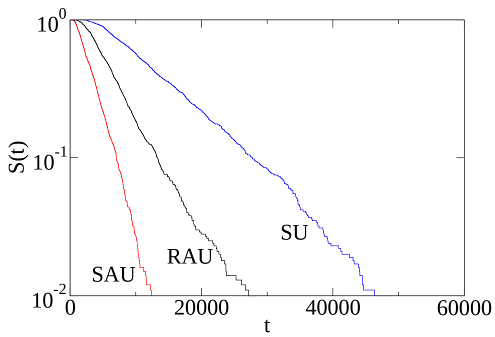

(e) Survival probability.

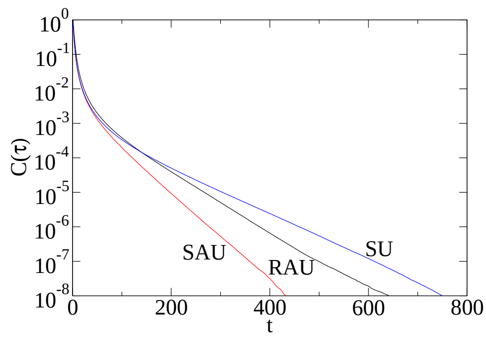

(f) Cumulative distribution of persistence times.

Figure 2.5: The voter model under the usual update rules (RAU, SAU, SU) on a **complete graph** for a system size $N = 10000$. All the averages where done over 1000 realizations.

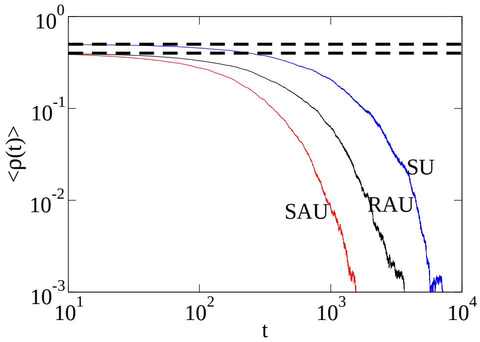

(a) Density of active links averaged over all runs in log-log scale. The different dashed lines stand for the different heights of the plateaus in the thermodynamic limit for the different update rules.

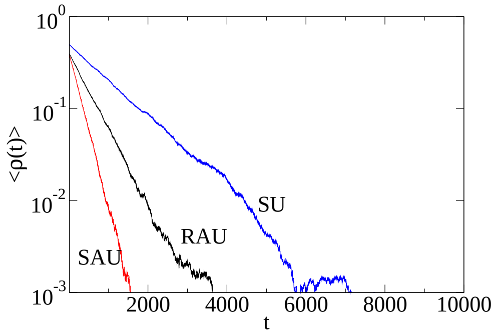

(b) Density of active links averaged over all runs in log-linear scale.

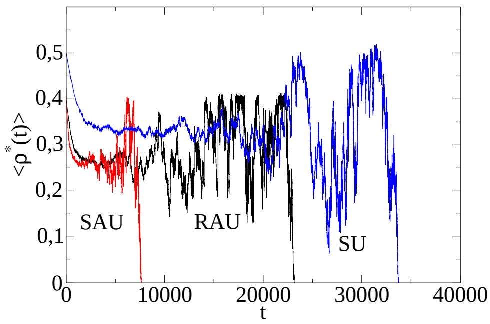

(c) Density of active links averaged over surviving runs.

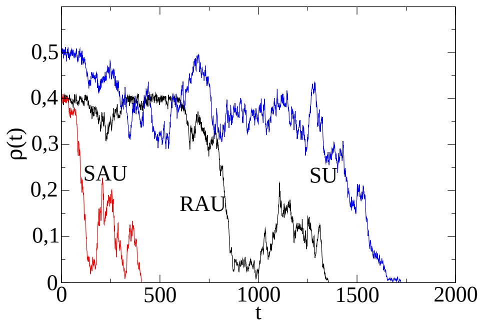

(d) Density of active links in single realizations.

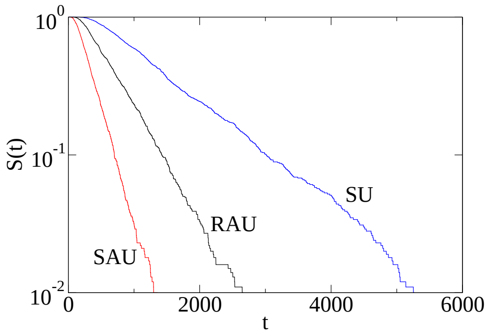

(e) Survival probability.

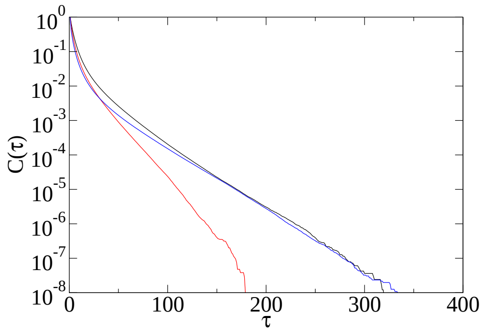

(f) Cumulative distribution of persistence times.

Figure 2.6: The voter model under the usual update rules (RAU, SAU, SU) on a **random graph** with average degree $\langle k \rangle = 6$ for a system size $N = 4000$. All the averages where done over 1000 realizations.

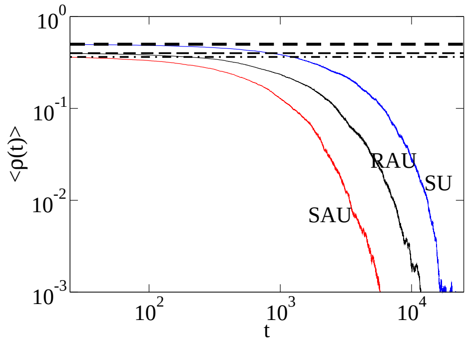

(a) Density of active links averaged over all runs in log-log scale. The different dashed lines stand for the different heights of the plateaus in the thermodynamic limit for the different update rules.

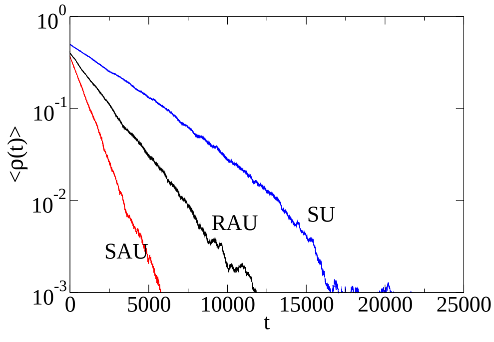

(b) Density of active links averaged over all runs in log-linear scale.

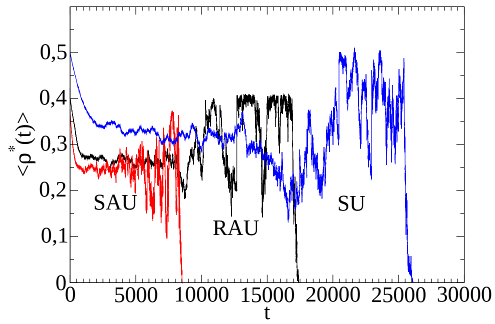

(c) Density of active links averaged over surviving runs.

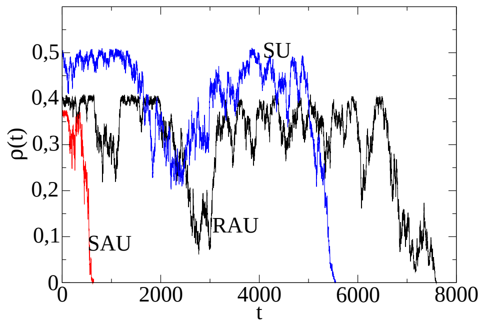

(d) Density of active links in single realizations.

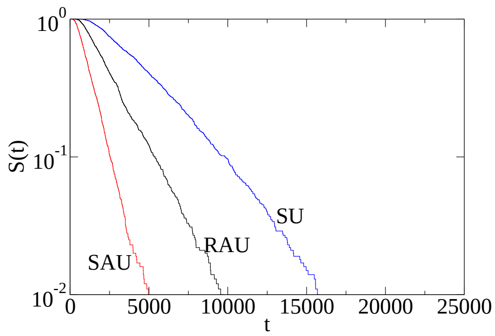

(e) Survival probability.

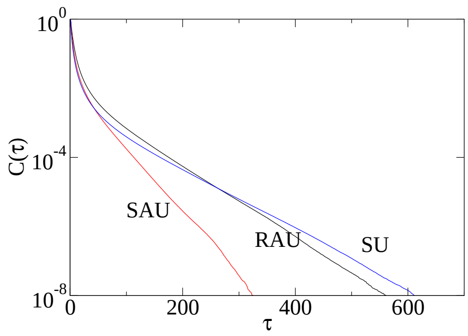

(f) Cumulative distribution of persistence times.

Figure 2.7: The voter model under the usual update rules (RAU, SAU, SU) on a **Barabási-Albert scale-free graph** with mean degree $\langle k \rangle = 6$ for a system size $N = 10000$. All the averages where done over 1000 realizations.

		RAU $\tau(N)$	SAU $\tau(N)$	SU $\tau(N)$
CG	$\langle\rho\rangle \| S(t)$	$N/2$	$0.23(4)N^{1.01(2)}$	$0.9(1)N^{1.01(2)}$
	C	$0.63(7)N^{0.47(2)}$	$0.33(4)N^{0.50(1)}$	$0.6(1)N^{0.51(2)}$
RG $\langle k\rangle = 6$	$\langle\rho\rangle \| S(t)$	$0.57(7)N^{0.99(2)}$	$0.34(6)N^{0.97(2)}$	$1.0(1)N^{1.01(2)}$
	C	$1.0(2)N^{0.47(2)}$	$0.38(6)N^{0.51(2)}$	$0.74(9)N^{0.51(2)}$
SFG $\langle k\rangle = 6$	$\langle\rho\rangle \| S(t)$	$0.25(5)N^{0.88(2)}$	$0.19(3)N^{0.92(5)}$	$1.6(4)N^{0.84(3)}$
	C	$0.35(7)N^{0.52(2)}$	$0.18(7)N^{0.53(4)}$	$1.0(3)N^{0.43(3)}$

Table 2.1: System size dependence of the characteristic times in the density of active links, $\langle\rho(t)\rangle$ and in the cumulative distribution of interevent times, $C(\tau)$, for different network topologies and node update rules. CG stands for complete graph, RG for random graph and S-FG for scale-free graph.

Our results indicate that the voter model has the same qualitative dynamical behaviour under RAU, SAU and SU node update rules. These results can be summarized as follows:

Density of active links:

$\langle\rho(t)\rangle$: For the ensemble average over all realizations we find an exponential decay in $\langle\rho(t)\rangle \propto e^{-t/\tau(N)}$ with a characteristic time that scales as $\tau(N) \propto N$ for a complete graph and random graphs. For the case of Barabási-Albert scale-free graphs the scaling is compatible with the analytical result $\tau(N) \propto N/\log(N)$ [2,18,20]. We can see that the characteristic time diverges with the system size, so that $\langle\rho(t)\rangle$ remains constant in the infinite size limit for any of these networks. This is telling us already that the system is not reaching an ordered state in the thermodynamic limit.

$\langle\rho^*(t)\rangle$: Decays exponentially until it reaches a plateau. The plateau height is independent of the system size, meaning that, on average, the realizations that have not yet reached an absorbing state, stay at a disordered state with a finite and large fraction of active links.

Survival probability:

$S(t)$: The survival probability decays exponentially, $S(t) \propto e^{-t/\tau(N)}$, with the same characteristic time as $\langle\rho(t)\rangle$. That's why when combining $\langle\rho(t)\rangle/S(t) = \langle\rho^*(t)\rangle$ we find a constant value for $\langle\rho^*(t)\rangle$. The mean times to reach consensus for finite systems are well defined. In the infinite size limit, as $\tau(N)$ diverges with the system size, we can conclude again that the system does not reach an ordered state and the survival probability is just equal to one for all times in the thermodynamic limit.

Cumulative distribution of persistence times:

$C(\tau)$: This distribution shows an exponential tail, indicating that there is a well defined average persistence time. The characteristic time in the exponential tail scales approximately as the square root of the system size.

These are the features shared by all standard node update rules. There are also differences, since the precise characteristic times and the plateau heights of $\langle \rho(t) \rangle$ and $\langle \rho^*(t) \rangle$ depend on the update rule. See Figs. 2.6a and 2.7a where the plateaus for the different update rules are plotted wit a dashed black line. It is clear that the difference between RAU and SAU update rule lies in correlations that will be present in SAU and not in RAU. For the case of SU, the differences come from the fact that for this update rule the dynamics is purely discrete. Still the main result is that the qualitative behavior is the same: for these three update rules the system remains, in the thermodynamic limit, in an active disordered configuration for the voter model dynamics in a complete graph and in complex networks of infinite effective dimensionality such as Erdös-Renyi and Barabási-Albert networks. Also the activity patterns are very homogeneous, with a well defined persistence time.

3

Update rules for heterogeneous activity patterns

3.1 Motivation: human activity patterns

Many interevent time distributions measured recently in empirical studies about human activities such as e-mail communication, surface mail, timing of financial trades, visits to public places, long-range travels, online games, response time of internauts, printing processes and phone calls among others [41, 42, 43, 44, 45, 46, 47, 48, 49, 50], show a heavy tail or a power law for large times. Some efforts have been made to unravel the origin as well as the consequences of such a particular timing in human activities. There exist mainly two important topics in which research is being done:

- Origin of these heavy-tailed distributions: in the literature one can find two main approaches
  - Explain these tails based on cyrcadian cycle and seasonality, via a non-homogeneous Poisson process with a cascading mechanism. [41, 48]
  - Root these heavy tails in the way individuals organize and prioritize their tasks modelling it via a priority queing model. [42, 45, 49, 50]
- Effects of this special timing on certain dynamics: independently of the origin of this feature it has been noticed that a non-homogeneous interaction in time can give rise to non-trivial behaviour. An example considered so far in some detail is spreading and infection dynamics: SI-type spreading dynamics have been investigated, showing that this peculiar timing gives rise to a slowing down of the dynamics that cannot be explained just by a change of time scale but it changes the functional form of the prevalence of a disease [44, 45, 46, 47].

The present work explores the second of these two big topics related to interevent time distributions. First we modify the update rule to account for this special pattern of activity and see whether it has an effect on the outcome of the dynamics or not, irrespective of the origin of such heavy tails. In order to do this we define an update rule and implement it in two different ways. One that is coupled to the dynamics of the states of the agents, *endogenous update*; and one that is independent of the states of the agents, *exogenous update*. Second, as an illustration, we apply the two variations of the new update rule to the voter model.

3.2 New update rule

A set of N agents are placed on the nodes of a network of interaction. Each agent i is characterized by its state x_i and an internal variable that we will call *persistence time* τ_i. For any given interaction model (Ising, voter, contact process, ...), the dynamics is as follows: at each time step,

1. with probability $p(\tau_i)$ each agent i becomes active, otherwise it stays inactive;
2. active agents update their state according to the dynamical rules of the particular interaction model;
3. all agents increase their persistence time τ_i in one unit

The persistence time measures the time since the last event for each agent. Typically an event is an interaction (*exogenous update*: active agents reset $\tau = 0$ after step (ii)) or a change of state (*endogenous update*: only active agents that change their state in step (ii) reset $\tau = 0$).
There are two interesting limiting cases of this update when $p(\tau)$ is independent of τ: when $p(\tau) = 1$, all agents are updated synchronously; when $p(\tau) = 1/N$, every agent will be updated on average once per N unit time steps. The latter corresponds to the usual random asynchronous update (RAU). We are interested in non-Poissonian activation processes, with probabilities $p(\tau)$ that decay with τ, that is, the longer an agent stays innactive, the harder is to activate. To be precise, we will later consider that

$$p(\tau) = \frac{b}{\tau} , \tag{3.1}$$

where b is a parameter that controls the decay with τ.
We expect the persistence $M(t)$ to be related to the activation probability $p(\tau)$. Neglecting the actual dynamics and assuming that at each update event, the agent changes state we can find an approximate relation between $M(t)$ and $p(\tau)$. Recall that $M(t)$ is the probability that an agent changes state (updating and changing state coincide in this approximation) t timesteps after her last change of state. Therefore the probability that an agent has not changed state in $t-1$ timesteps is $1 - \sum_{j=1}^{t-1} M(j)$ and the probability of changing state having persistence time t is

$p(t)$. Therefore we can write:

$$\left(1 - \sum_{j=1}^{t-1} M(j)\right) p(t) = M(t), \tag{3.2}$$

with $p(1) = M(1)$. Taking the continous limit and expressing this equation in terms of the cumulative persistence distribution we obtain

$$d\ln(C(t)) = -p(t)dt. \tag{3.3}$$

Setting $p(\tau) = b/\tau$ the cumulative persistence distribution decays as a power law $C(t) \sim t^{-\beta}$ with $\beta = b$. Numerical simulations show that this approximation holds for the voter model on a fully connected network for endogenous updates and for a small range of b-values in the exogenous update for any topology of the ones considered in this study.
The modification of the model is investigated more exhaustively for the case in which the cumulative persistence is set to a power law $C(\tau) \propto \tau^{-\beta}$, but any distribution $C(\tau)$ can be plugged into the definition of $p(\tau)$, Eq. (3.3). In fact the case $\beta = 1$ will be studied in more detail.

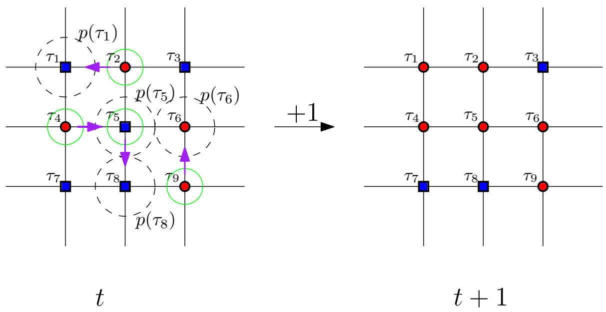

Figure 3.1: Example of the new update rule. Every agent gets updated with her own probability $p(\tau_i)$, being τ_i her persistence time.

When applied to the voter model the new update rule we changes the transition rates for node-dependent rates that are function of the persistence time of each node. A precedent of our study is the work in ref. [51], where they just modified the transition rates in the simplest way, in order to see if it had any effect on the mean times to reach consensus. In the present work we use a variation that leads to the appearance of heavy tails in the persistence $M(\tau)$ and we focus on the question of the implication of the update rule on the existence or not of coarsening.

3.3 Voter model with exogenous update

If instead of the standard update rules discussed in section 2.2 we now use the exogenous version of the new update, the agents will not be characterized only by

its state x_i, but also by their internal time τ_i, *i.e.* the time since their last update event.
The simulation steps for this modified voter model are as follows:

1. With probability $p(\tau_i)$ every agent i is given the opportunity of updating her state by interacting with a neighbor.

2. If the agent interacts, one of its neighbours j is chosen at random and agent i copies j's state. $x_i \to x_i = x_j$. Agent i resets $\tau_i = 0$.

3. The time is updated to a unit more and we return to 1 to keep on with the dynamics.

For an activation probability $p(\tau) = 1/\tau$, *i.e.* $\beta = 1$ we ran simulations on a complete graph, Fig. 3.2, on random graphs of different average degrees, Fig. 3.3, and on a Barabási-Albert scale-free graph of average degree $\langle k \rangle = 6$, Fig. 3.4 and for different system sizes.

Our results can be summarized as follows:

Density of active links $\langle \rho(t) \rangle$ and $\langle \rho^*(t) \rangle$: When averaged over all runs, $\langle \rho(t) \rangle$ decays with different rates depending on the interaction networks and system sizes. For bigger system sizes the decay slows down, reaching a plateau in the thermodynamic limit (Figs. 3.2a,3.3a and 3.4a). When averaged over active runs $\langle \rho^*(t) \rangle$ reaches a plateau (Figs. 3.2b,3.3b and 3.4b), which is independent of the system size, showing that living runs stay, on average, on a dynamical disordered state, as happens with standard update rules.

Survival probability $S(t)$: It is one until it decays in a nontrivial way. It is not a purely exponential decay, but decays faster than any power law, therefore no normalization problems are expected.

Cumulative persistence $C(\tau)$: Develops a power-law tail consistent with the exponent $\beta = b$, which in this case is set to 1, as we could expect if the approximation of Eq.3.3 holds.

The dynamics does not order the system with the exogenous update.

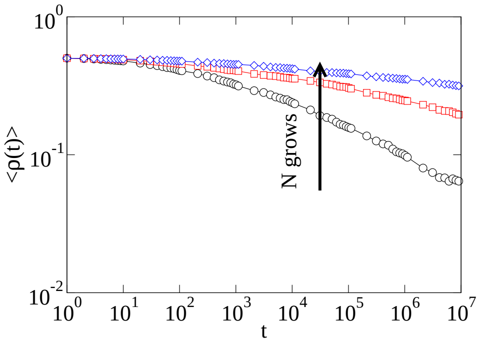

(a) Density of active links averaged over all runs.

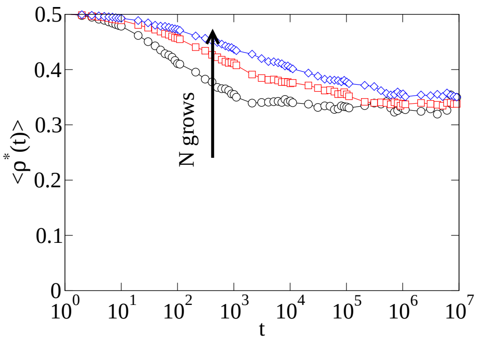

(b) Density of active links averaged over surviving runs.

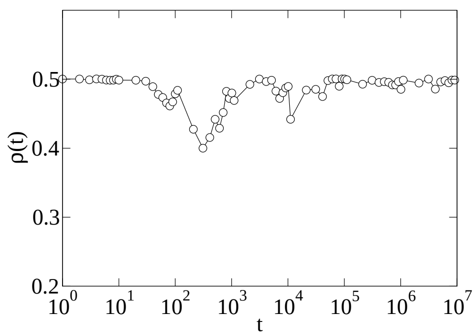

(c) Density of active links in a single realization with system size $N = 10^3$.

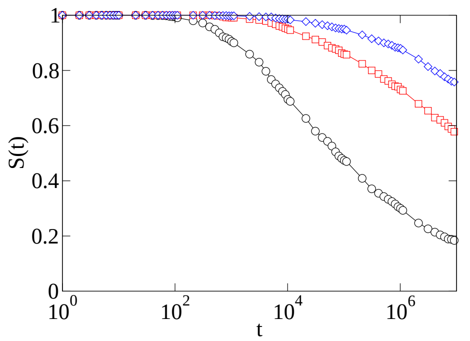

(d) Survival probability.

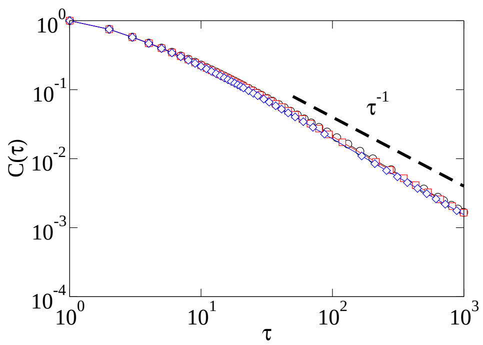

(e) Cumulative distribution of persistence times.

Figure 3.2: Results of the voter model under the exogenous update rule with activation probability $p(\tau) = 1/\tau$ on a complete graph. Different colors stand for different system sizes $N = 100, 200, 300$. All the averages are done over 1000 realizations. Larger system sizes display the same behavior, but the characteristic times are much longer, and so are the simulations.

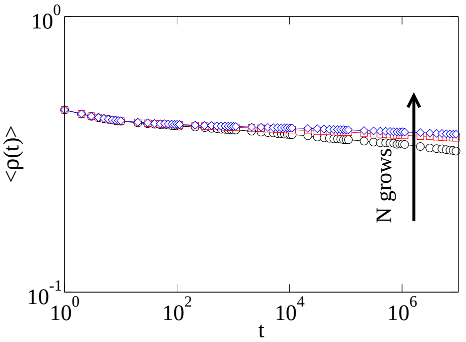

(a) Density of active links averaged over all runs.

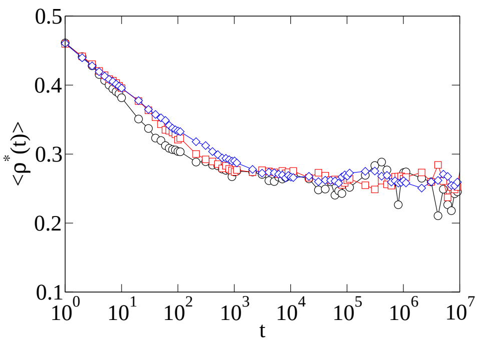

(b) Density of active links averaged over surviving runs.

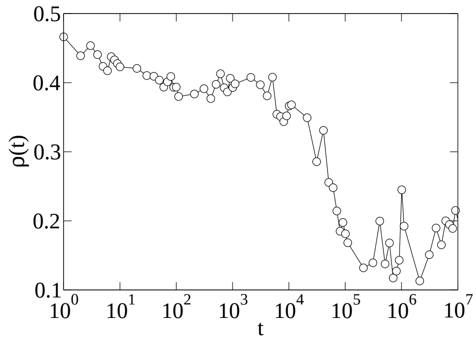

(c) Density of active links in a single realization with system size $N = 4000$.

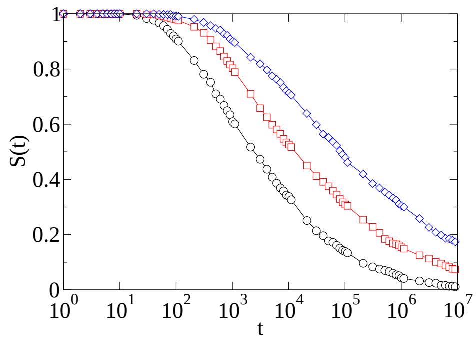

(d) Survival probability.

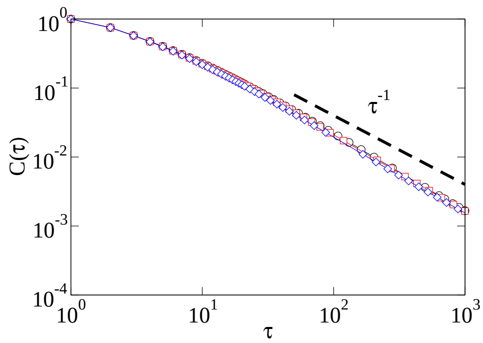

(e) Cumulative distribution of persistence times.

Figure 3.3: Results of the voter model under the exogenous update rule with activation probability $p(\tau) = 1/\tau$ on a random graph with $\langle k \rangle = 6$. Different colors stand for different system sizes $N = 1000, 2000, 3000$ for $\langle \rho(t) \rangle$ and $C(\tau)$; and $N = 100, 200, 300$ for $\langle \rho^*(t) \rangle$ and $S(t)$, otherwise the plateau in $\langle \rho^*(t) \langle$ and the decay $S(t)$ are not present in a reasonable simulation time. All the averages are done over 1000 realizations.

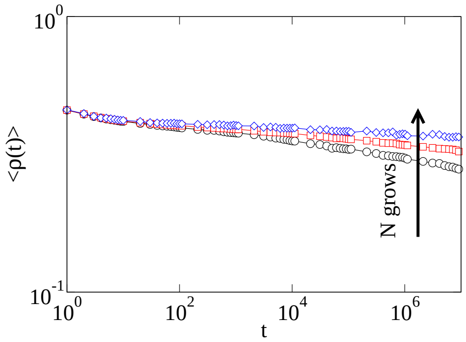

(a) Density of active links averaged over all runs.

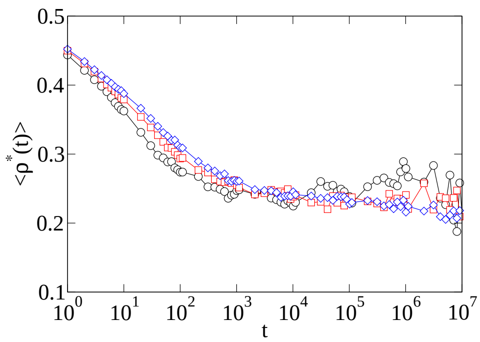

(b) Density of active links averaged over surviving runs.

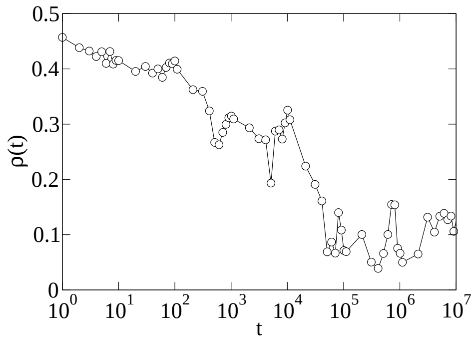

(c) Density of active links in a single realization with system size $N = 10^4$.

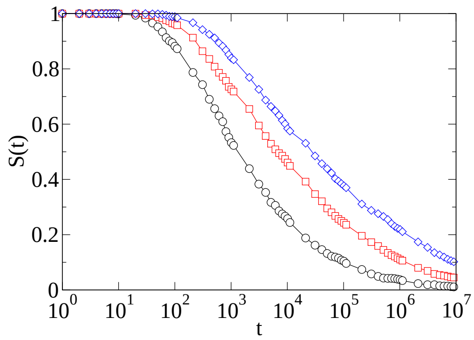

(d) Survival probability.

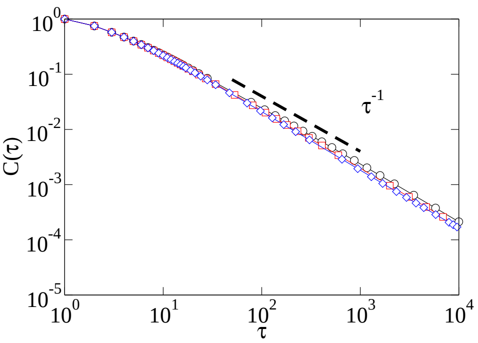

(e) Cumulative distribution of persistence times.

Figure 3.4: Results of the voter model under the endogenous update rule with activation probability $p(\tau) = 1/\tau$ on a scale-free graph with mean degree $\langle k \rangle = 6$. Different colors stand for different system sizes $N = 1000, 2000, 3000$ for $\langle \rho(t) \rangle$ and $C(\tau)$; and $N = 100, 200, 300$ for $\langle \rho^*(t) \rangle$ and $S(t)$, otherwise the plateau in $\langle \rho^*(t) \langle$ and the decay $S(t)$ are not present in a reasonable simulation time. All the averages are done over 1000 realizations.

3.4 Voter model with endogenous update rule

We now use the endogenous update for the voter mopdel. This is just the same as the exogenous update rule, but in this case the internal time of each agent i, τ_i, is the time since her last change of state. In this way the update rule is coupled to the states of the agents.
The simulation steps for the modified voter model that we study are as follows:

1. With probability $p(\tau_i)$ every agent i is given the opportunity of updating her state by interacting with a neighbor.

2. If the agent interacts, one of its neighbours j is chosen at random and agent i copies j's state. $x_i \to x_i = x_j$.

3. If the update produces a change of state of node i, then τ_i is set to zero.

4. The time is updated to a unit more and we return to 1 to keep on with the dynamics.

The question now is if this modification will lead to qualitative changes in the outcome of the dynamics of the voter model. For an activation probability $p(\tau) = 1/\tau$, *i.e.* $\beta = 1$ we ran simulations on a complete graph, Fig. 3.5, on random graphs of different average degrees, Fig. 3.6, and on a Barabási-Albert scale-free graph of average degree $\langle k \rangle = 6$, Fig. 3.7 and for different system sizes. The exponents in the power laws of the quantities plotted in figures 3.5-3.7 are summarized in table (3.1) for the cases of complete, random and scale-free graph with mean degree $\langle k \rangle = 6$.

	$\langle \rho(t) \rangle \propto t^{-\gamma}$	$S(t) \propto t^{-\delta}$	$C(\tau) \propto t^{-\beta}$
Complete graph	$\gamma = 0.985(5)$	$\delta = 0.95(2)$	$\beta = 0.99(3)$
Random graph $\langle k \rangle = 20$	$\gamma = 0.99(1)$	$\delta = 0.82(1)$	$\beta = 0.94(4)$
Random graph $\langle k \rangle = 6$	$\gamma = 0.249(4)$	$\delta = 0.13(1)$	$\beta = 0.45(1)$
Scale-free graph $\langle k \rangle = 6$	$\gamma = 0.324(7)$	$\delta = 0.32(1)$	$\beta = 0.46(1)$

Table 3.1: Exponents for the power-law decaying quantities $\rho(t)$, $S(t)$ and $C(\tau)$ for the voter model with the endogenous update rule.

We can see from the table that, increasing the average degree of the random networks we get results that get closer to the ones on a complete graph.
Our results can be summarized as follows:

Density of active links $\langle \rho(t) \rangle$ *and* $\langle \rho^*(t) \rangle$*:* When averaged over all runs, $\langle \rho(t) \rangle$ decays as a power law with different exponents depending on the interaction network. When averaged over active runs $\langle \rho^*(t) \rangle$ we see that it decays as a power-law until it reaches a plateau whose height depends on the system

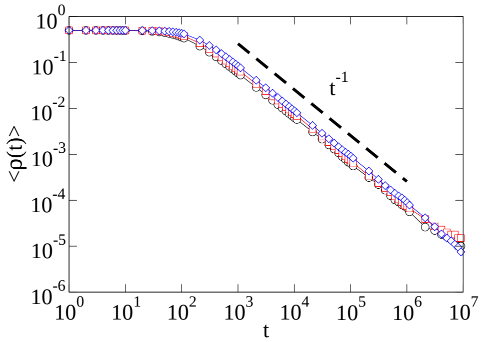

(a) Density of active links averaged over all runs.

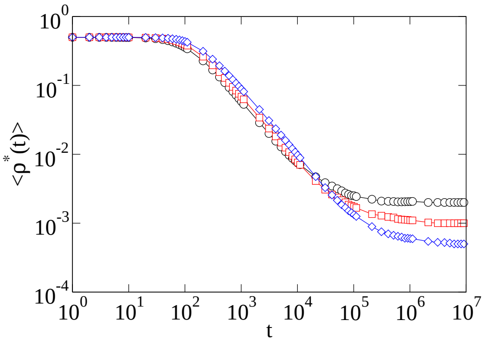

(b) Density of active links averaged over surviving runs.

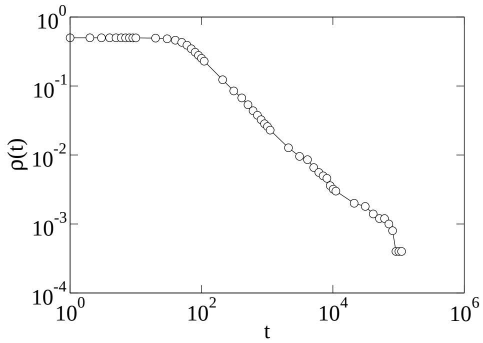

(c) Density of active links in a single realization with system size $N = 10^4$.

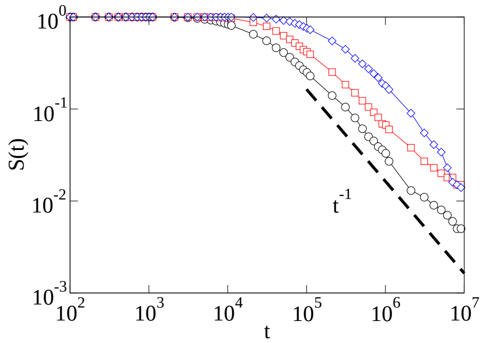

(d) Survival probability.

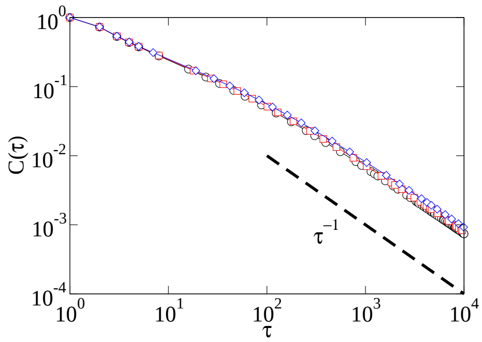

(e) Cumulative distribution of persistence times.

Figure 3.5: Results of the voter model under the endogenous update rule with activation probability $p(\tau) = 1/\tau$ on a complete graph. Different colors stand for different system sizes $N = 1000, 2000, 4000$. All the averages are done over 1000 realizations.

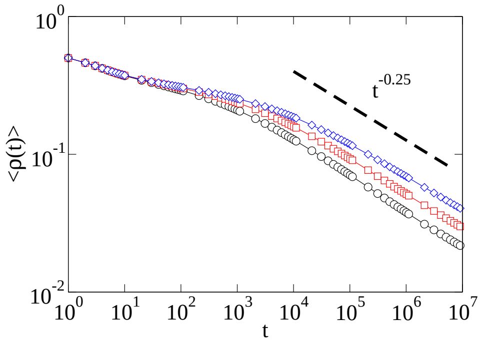

(a) Density of active links averaged over all runs.

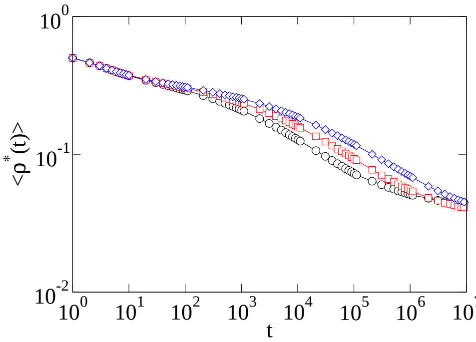

(b) Density of active links averaged over surviving runs.

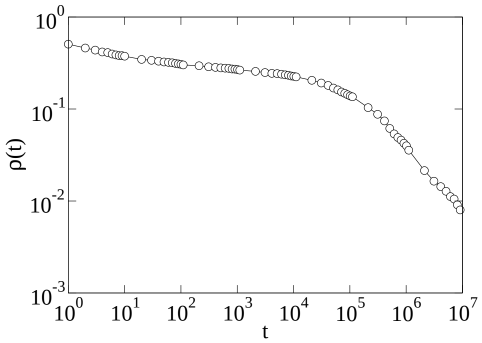

(c) Density of active links in a single realization with system size $N = 4000$.

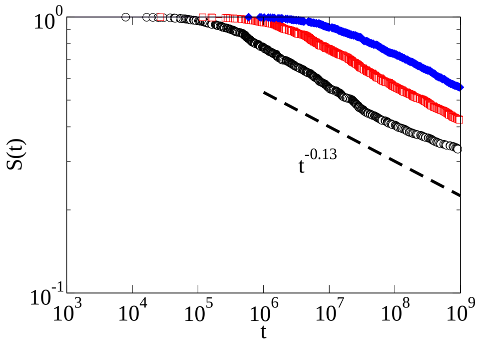

(d) Survival probability.

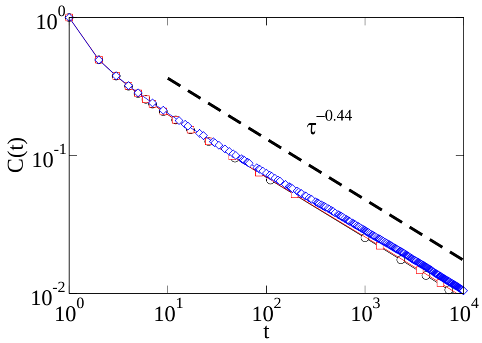

(e) Cumulative distribution of persistence times.

Figure 3.6: Results of the voter model under the endogenous update rule with activation probability $p(\tau) = 1/\tau$ on a random graph with $\langle k \rangle = 6$. Different colors stand for different system sizes $N = 1000, 2000, 4000$. All the averages are done over 1000 realizations.

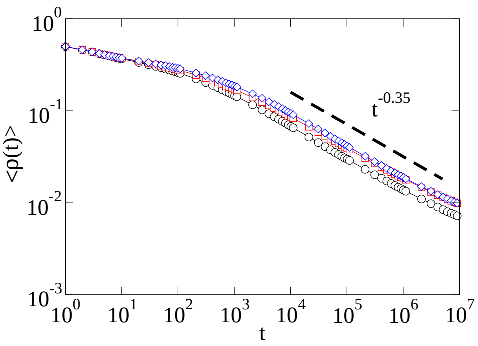

(a) Density of active links averaged over all runs.

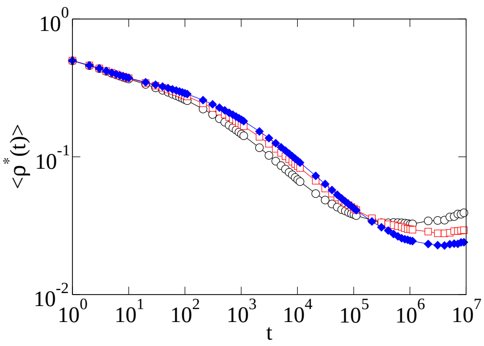

(b) Density of active links averaged over surviving runs.

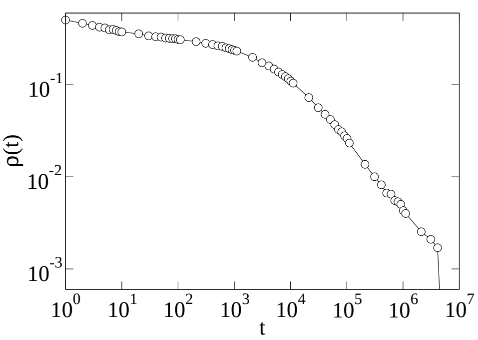

(c) Density of active links in a single realization with system size $N = 10^4$.

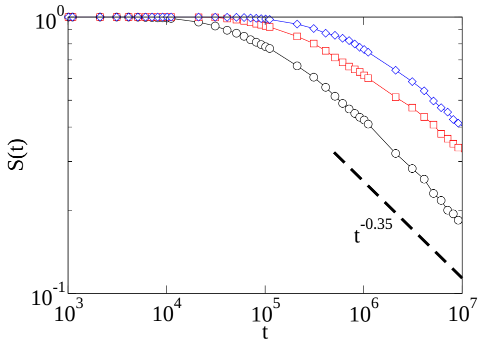

(d) Survival probability.

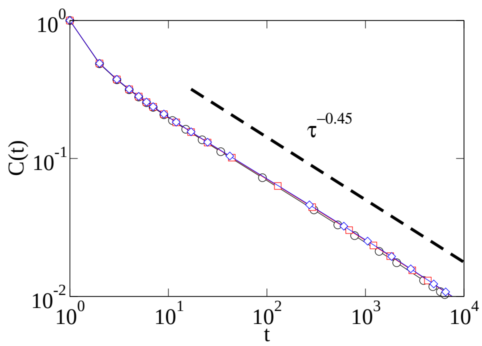

(e) Cumulative distribution of persistence times.

Figure 3.7: Results of the voter model under the endogenous update rule with activation probability $p(\tau) = 1/\tau$ on a scale-free graph with mean degree $\langle k \rangle = 6$. Different colors stand for different system sizes $N = 1000, 2000, 4000$. All the averages are done over 1000 realizations.

size and is smaller for bigger system sizes, which tells that **the system is heading towards consensus**, contrary to what happens with the standard update rules. This is one of the main results of the present work.

Survival probability $S(t)$: It is one until it decays, also like a power-law. The exponents are in all cases smaller or around 1, so that **the average time to reach consensus diverges for all system sizes**. Remember that the mean time to reach consensus is $\langle T \rangle = \int_0^\infty S(t)dt$. So, we cannot speak of a properly defined average time to reach consensus.

Cumulative persistence $C(\tau)$: Develops a power-law tail. For a complete graph and a random network with high degree we recover an exponent β in the tail of the interevent times cumulative distribution $C(\tau)$ that matches the one we wanted it to follow given our calculations and our choice $p(\tau) = 1/\tau$. For the other two networks, random and scale-free with $\langle k \rangle = 6$ we recover that the tail behaves aproximately as $1/\sqrt{\tau}$.

The dynamics does not order the system with the endogenous update through a coarsening process that leads to the divergence of the mean time to reach consensus for all system sizes. As a summary, the complete graph case gives us already the qualitative behavior: for the voter model with exogenous update the timescales are much larger than in the voter model with RAU, but it has the same qualitative behavior: the system doesn't order in the thermodynamic limit, but stays in a disordered dynamical configuration with asymptotic coexistence of both states. This contrasts with what happens with the endogenous update, where the timescales are also perturbed, but with the difference that a coarsening process occurs, slowly ordering the system. We have checked that the ensemble average of the magnetization $\langle m(t) \rangle = \frac{1}{N}\sum_{i=1}^{N} \langle s_i(t) \rangle$ is conserved for the exogenous update, whereas for the endogenous update this conservation law breaks down, as previously discussed in Ref. [51]. The non-conservation of the magnetization leads to an ordering process. The conservation law is broken due to the different average values of the persistence time in both populations of agents (+1 and -1) leading to different average activation probabilities.

3.5 Varying the exponents of the cumulative persistence $C(\tau)$

As we saw in section 3.2 the exponent in the persistence times cumulative distribution $C(\tau) \propto \tau^{-\beta}$ should be related to the parameter b appearing in the activation probability $p(\tau) = b/\tau$. If every time we let an agent be updated, this one changes state, this relation is such that $\beta = b$. When introducing the dynamics, this relation is not so clear and depends also on the kind of network where the dynamics are taking place. In Fig. 3.8 we can see the interevent times cumulative distributions for different values of b for the exogenous update.

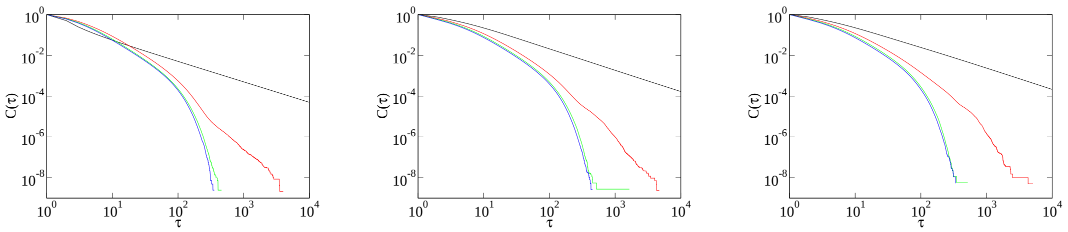

(a) Cumulative persistence for different b's on a complete graph.

(b) Cumulative persistence for different b's on a random graph with $\langle k \rangle = 6$.

(c) Cumulative persistence for different b's on a Barabási-Albert scale-free network with $\langle k \rangle = 6$.

Figure 3.8: Endogenous update: cumulative persistence $C(\tau)$ for different values of the parameter b (grows from left to right) appearing in the activation probability $p(\tau)$ for complete graph, random graph with $\langle k \rangle = 6$ and Barabási-Albert scale-free network with $\langle k \rangle = 6$ and for system size $N = 1000$.

We can see that for $b = 1$ the power law tail is recovered with an exponent that matches $\beta = b$. For higher values of b the form of the tail is rapidly lost and we have cumulative persistences $C(\tau)$ are similar to those with standard update rules, *i.e.*, do not display heavy tails.
In Fig. 3.9 we can see the interevent times cumulative distributions for different values of b for the endogenous update.

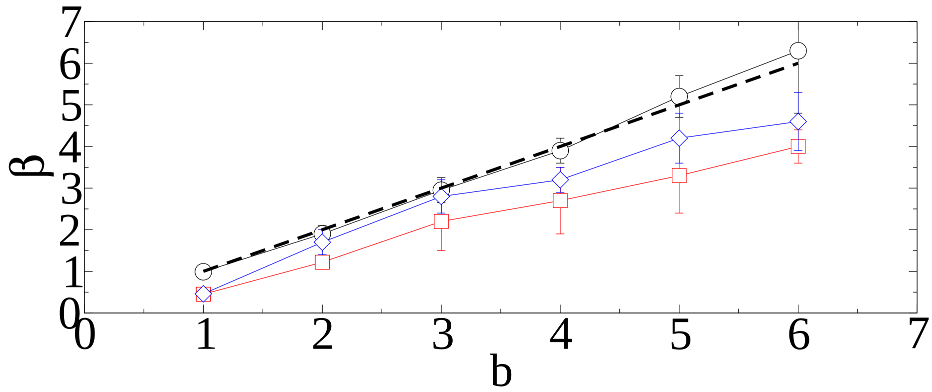

Figure 3.10: Endogenous update. Relation of β, the exponent of the cumulative persistence distribution $C(t) \sim t^{-\beta}$, and b, the parameter in the function $p(\tau) = b/\tau$ for three different topologies; fully connected (circles), random with $\langle k \rangle = 6$ (squares) and scale free with $\langle k \rangle = 6$ (diamonds) networks. As a guide to the eye we plot the curve $\beta = b$ with a dashed line.

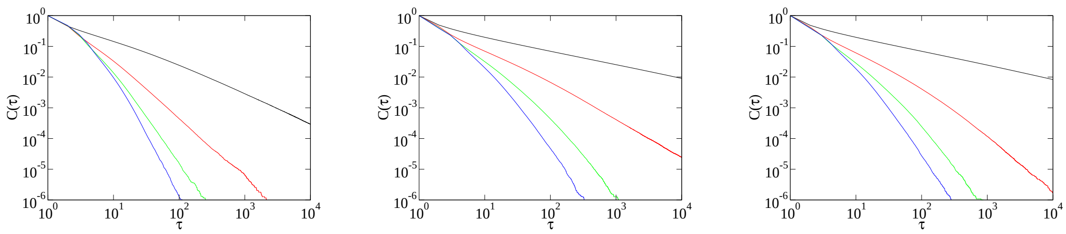

(a) Cumulative persistence for different b's on a complete graph.

(b) Cumulative persistence for different b's on a random graph with $\langle k \rangle = 6$.

(c) Cumulative persistence for different b's on a Barabási-Albert scale-free network with $\langle k \rangle = 6$.

Figure 3.9: Endogenous update: cumulative persistence $C(\tau)$ for different values of the parameter b (grows from left to right) appearing in the activation probability $p(\tau)$ for complete graph, random graph with $\langle k \rangle = 6$ and Barabási-Albert scale-free network with $\langle k \rangle = 6$ and for system size $N = 1000$.

The endogenous update rule has a wider range of b-values for which the heavy tail is recovered. We measured the exponents of the tails for different values b in the different topologies. The results can be seen in Fig. 3.10

Surprisingly, for the case of the complete graph, we recover the relation predicted, *i.e.* a linear relation between β in the cumulative distribution function and b, the parameter in the probability $p(\tau)$.
In the case of other topologies we find that the relation $b-\beta$ is not the one predicted in the case of no interactions, but it displays a reminiscent behaviour of the one observed for a complete graph: the exponent β found in the cumulative interevent time distribution increases monotonically with the parameter b in the activation

probability.

4

Conclusions

Specific conclusions

Standard update rules. With the standard update rules; RAU, SAU and SU; the voter model on the networks studied here behaves qualitatively the same. In terms of consensus formation and in the thermodynamic limit, the model reaches asymptotically a stationary active state with coexistence of agents in both states. For finite size systems the average density of interfaces $\langle\rho(t)\rangle$ and the survival probability $S(t)$ decay exponentially with a characteristic time that scales as N for any of these updates on a complete graph and on a random graph, but as something compatible with $N/\ln(N)$ on Barabási-Albert networks. The patterns of interaction, measured via the interevent times distribution $M(\tau)$ or, equivalently the cumulative interevent time ditribution $C(\tau)$ appear to be quite homogeneous. $C(\tau)$ shows an exponential tail, which has a characteric time that scales approximately as $\sqrt{N}$.

New update rule. With the exogenous update the model behaves qualitatively the same as with standard update rules, *i.e.*, although the timescales are disturbed in a non-trivial way, the system does not reach order in the thermodynamic limit for any of the topologies considered. We are able to reproduce heavy tails in the cumulative persistence $C(\tau)$ for small values of the parameter b appearing in the activation probability $p(\tau) = b/\tau$.
With the endogenous version of the new update rule, and using an activation probability $p(\tau) = 1/\tau$ the voter model undergoes a coarsening process that in the thermodynamic limit orders the system asymptotically. The coarsening process is such that the average density of interfaces $\langle\rho(t)\rangle$ decays as a power law with different exponents depending on the interaction network. The survival probability also decays in a power-law manner whith an exponent smaller than one in any of the interaction networks that were studied. This fact makes the average time to reach consensus to be not well defined. Regarding the interaction patterns, these are very heterogeneous, having $C(\tau)$ a heavy tail, consistent with a power law of different

exponents depending on the interaction network. For the case of a complete graph we can even approximately infer the exponent in the tail of $C(\tau) \propto \tau^{-\beta}$ given the activation probability $p(\tau) = b/\tau$, having $\beta = b$.

General conclusions.

As a general conclusion, we have implemented an update rule in two ways to the voter model, which is able to account for heterogeneous activity patterns. When the update rule is coupled to the states of the agents (endogenous update) it happens to give qualitatively different results than the one known for the voter model with the standard update rules. For the state-dependent update rule (endogenous update), the system orders in the thermodynamic limit while it stayed in a disordered active state for the standard update rules in infinite dimensional networks. Also the times to reach consensus are varied in such a way that for the endogenous version of the update rule they are not well defined. It is then something to take into account when drawing conclussions from microscopic models of human activity, that the macroscopic outcome might vary depending on the timing and sequences of the interactions. Even if we implement this characteristic in the model, the way in which it is done can have different results (exogenous vs endogenous update rule). Recent research on human dynamics has revealed the "small but slow" paradigm [46, 45], that is, the spreading of an infection can be slow despite the underlying small-world property of the underlying network of interaction. Here, with the help of the general updating algorithm for agent based models which can account for realistic interevent time distributions, we have shown that the competition of opinion can lead to slow ordering not only in small networks but also in the mean field case. The results provide a theoretical framework that bridges the empirical efforts devoted to uncover the properties of human dynamics with modeling efforts in opinion dynamics.

A

Interaction networks

The interaction networks where the model is studied are the graphs schematically shown in figs. (A.1)-(A.3).

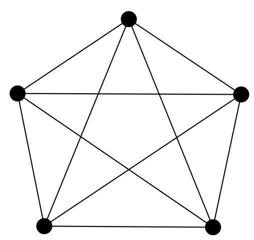

Figure A.1: Complete graph.

Complete graph: Every node in the network is connected to all the other nodes. This is what is also called all-to-all interactions.

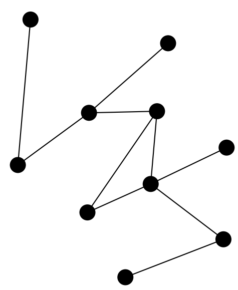

Figure A.2: Random graph.

Random graph: They are also called Erdös-Renyi graphs. We have a set of N nodes. There is a probability p that each of the $N(N-1)/2$ possible links among them exists. Usually the probability p is set such that, given a system size N, the average degree $\langle k \rangle$, *i.e.* the average number of neighbours of a node, of the network is fixed, then $\langle k \rangle = pN(N-1)/2$.

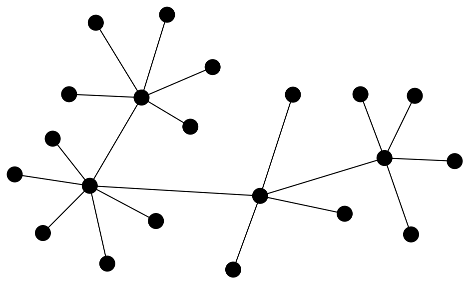

Figure A.3: Scale-free graph.

Scale-free graph: The main characteristic of these kind of networks is that the degree distribution is a power-law. This fact enables the existence of hubs, *i.e.* extremely highly connected nodes. We generate here these networks using the method of Barabási-Albert, which consists of two ingredients: a growing network and the fact that new added nodes attach preferentially to high degree nodes. The main characteristic of these networks is their power-law degree distribution[1] $P(k) \propto k^{-\gamma}$ with exponent $\gamma = 3$.

For a general review on complex networks and related topics see [31].

[1]The degree distribution $P(k)$ of a network is the probability that a randomly chosen node has degree k.

Bibliography

[1] R. Holley, T.M. Liggett, Ergodic theorems for weakly interacting infinite systems and the voter model, Annals of Probability 3(4) (1975) 643–663.

[2] K. Suchecki, V.M. Eguíluz, M. San Miguel, Conservation laws for the voter model in complex networks, Europhysics Letters Journal B 69 (2005) 228.

[3] K. Suchecki, V.M. Eguíluz, M. San Miguel, Voter model dynamics in complex networks: Role of dimensionality, disorder and degree distribution, Physical Review E 72 (2005) 036132.

[4] S. Galam, Minority opinion spreading in random geometry, The European Physical Journal B - Condensed Matter and Complex Systems 25 (2002) 403–406.

[5] C. J. Tessone, R. Toral, P. Amengual, H. Wio, M. San Miguel, Neighborhood models of minority opinion spreading, European Physical Journal B 39.

[6] G. Deffuant, D. Neau, F. Amblard, G. Weisbuch, Mixing beliefs among interacting agents, Advances in Complex Systems 3 (2000) 87–98.

[7] R. Hegselmann, U. Krause, Opinion dynamics and bounded confidence: models, analysis and simulation, Journal of Artificial Societies and Social Simulation 5.

[8] R. Axelrod, The dissemination of culture: A model with local convergence and global polarization, Journal of Conflict Resolution 41.

[9] E. Ben-Naim, L. Frachebourg, P. L. Krapivsky, Coarsening and persistence in the voter model, Phys. Rev. E 53 (4) (1996) 3078–3087.

[10] M.A. Nowak, R.M. May, Evolutionary games and spatial chaos, Nature (London) 359 (1992) 826–829.

[11] B.A. Huberman, N.S. Glance, Evolutionary games and computer simulations, PNAS 90 (1993) 7716–7718.

[12] M. San Miguel, V.M. Eguíluz, R. Toral, K. Klemm, Binary and multivariate stochastic models of consensus formation, Computing in Science & Engineering 7 (2005) 67–73.

[13] C. Castellano, S. Fortunato, V. Loreto, Statistical physics of social dynamics, Review of Modern Physics 81 (2009) 591.

[14] P. Clifford, A. Sudbury, A model for spatial conflict, Biometrika 60(3) (1973) 581–588.

[15] C. Castellano, V. Loreto, A. Barrat, F. Cecconi, D. Parisi, Comparison of voter and glauber ordering dynamics on networks, Physical Review E 71 (2005) 066107.

[16] C. Castellano, D. Vilone, A. Vespignani, Incomplete ordering of the voter model on small-world networks, Europhys. Lett. 63 (1) (2003) 153–158.

[17] M.A. Serrano, K. Klemm, F. Vázquez, V.M. Eguíluz, M. San Miguel, Conservation laws for voter-like models on random directed networks, Journal of Statistical Mechanics: Theory and Experiment (2009) P10024.

[18] F. Vázquez, V.M. Eguíluz, Analytical solution of the voter model on uncorrelated networks, New Journal of Physics 10 (2008) 063011.

[19] E. Pugliese, C. Castellano, Heterogeneous pair approximation for voter models on networks, Europhysics Letters 88 (2010) 58004.

[20] V. Sood, S. Redner, Voter model on heterogeneous graphs, Physical Review Letters 94 (2005) 178701.

[21] F. Slanina, H. Lavicka, Analytical results for the sznajd model of opinion formation, The European Physical Journal B 35 (2003) 279–288.

[22] R. K. Pathria, Statistical mechanics, Butterworth-Heinemann, 1996.

[23] M. Plischke, B. Bergersen, Equilibrium statistical physics, World Scientific, 2006.

[24] J. M. Yeomans, Statistical mechanics of phase transitions, Clarendon Press, 1992.

[25] J. Cox, D. Griffeath, Diffusive clustering in the two dimensional voter model, Annals of Probability 14(2) (1986) 347–370.

[26] T.M. Liggett, Interacting particle systems, Springer Verlag, New York,NY, USA, 1985.

[27] T.M. Liggett, Stochastic interacting systems: contact, voter and exclusion processes, Springer Verlag, Berlin, Germany, 1999.

[28] L. Frachebourg, P.L. Krapivsky, Exact results for kinetics of catalytic reactions, Physical Review E 53(4) (1996) R3009.

[29] R.J. Glauber, Time-dependent statistics of the ising model, Journal of Mathematical Physics 4(2) (1963) 294.

[30] J. Cox, Coalescing random walks and voter model consensus times on the torus in $\mathbb{Z}^d$, Ann. Probab. 17 (4) (1989) 1333–1366.

[31] R. Albert, A.-L. Barabási, Statistical mechanics of complex networks, Rev. Mod. Phys. 74 (1) (2002) 47–97.

[32] M. E. J. Newman, S. H. Strogatz, D. J. Watts, Random graphs with arbitrary degree distributions and their applications, Phys. Rev. E 64 (2) (2001) 026118.

[33] D.J. Watts, S.H. Strogatz, Collective dynamics of “small-world” networks, Nature 393 (2) (1998) 440–442.

[34] D. Vilone, C. Castellano, Solution of voter model dynamics on annealed small-world networks, Phys. Rev. E 69 (1) (2004) 016109.

[35] M. Barthélémy, L. A. N. Amaral, Small-world networks: Evidence for a crossover picture, Phys. Rev. Lett. 82 (15) (1999) 3180–3183.

[36] D. Conforth, D.G. Green, D. Newth, Ordered asynchronous processes in multi-agent systems, Physica D 204 (2005) 70–82.

[37] E.D. Lumer, G. Nicolis, Synchronous versus asynchronous dynamics in spatially distributed systems, Physica D 71 (1994) 440–452.

[38] E. Alba, M. Giacobini, M. Tomassini, S. Romero, Comparing synchronous and asynchronous cellular genetic algorithms, in: Parallel Problem Solving from Nature - PPSN VII, volume 2439 of Lecture Notes in Computer Science, Springer Verlag, 2002, pp. 601–610.

[39] B. Schönfisch, A. de Roos, Synchronous and asynchronous updating in cellular automata, BioSystems 51 (1999) 123–143.

[40] M.A. Nowak, S. Bonhoeffer, R.M. May, More spatial games, International Journal of Bifurcation and Chaos 4(1) (1994) 33–56.

[41] R.D. Malmgren, D.B. Stouffer, A.S.L.O. Campanharo, L.A.N. Amaral, On universality in human correspondence activity, Science 325 (2009) 1696.

[42] J. Gama Oliveira, A.-L. Barabási, Darwin and einstein correspondence patterns, Nature 437 (2005) 1251.

[43] J.-P. Eckmann, E. Moses, Danilo Sergi, Entropy dialogues creates coherent structures in e-mail traffic, Science 325 (2009) 1696.

[44] J.L. Iribarren, E. Moro, Impact of human activity patterns on the dynamics of information diffusion, Physical Review Letters 103 (2009) 038702.

[45] A. Vázquez, B. Rácz, A. Lukács, A.-L. BArabási, Impact of non-poissonian activity patterns on spreading processes, Physical Review Letters 98 (2007) 158702.

[46] M. Karsai, M. Kivelä, R.K. Pan, K. Kaski, J. Kertész, A.-L. Barabási, J. Saramäki, Small but slow world: how network topology and burstyness slow down spreading, arXiv [physics.soc-ph] 1006.2125v3.

[47] B. Min, K.-I. Goh, A. Vázquez, Spreading dynamics following human activity patterns, arXiv [physics.dat-an] 1006.2643v2.

[48] R.D. Malmgren, D.B. Stouffer, A.E. Motter, L.A.N. Amaral, A poissonian explanation for heavy tails in e-mail communication, PNAS 105 (2008) 18153–18158.

[49] A.-L. Barabási, The origin of bursts and heavy tails in human dynamics, Nature 435 (2005) 207–211.

[50] A. Vázquez, J. Gama Oliveira, Z. Dezsö, K.-I. Goh, I. Kondor, A.-L. Barabási, Modeling bursts and heavy tails in human dynamics, Physical Review E 73 (2006) 036127.

[51] H.-U. Stark, C.J. Tessone, F. Schweitzer, Decelerating microdynamics can accelerate macrodynamics in the voter model, Physical Review Letters 101 (2008) 018701.